Diffusive CH_4 fluxes from aquaculture ponds using floating chambers and thin boundary layer equations

Ping Yang[a,b,1], Jiafang Huang[a,b,1], Hong Yang[c,d,e,1], Josep Peñuelas[f,g], Kam W. Tang[h], Derrick Y.F. Lai[i*], Dongqi Wang[j], Qitao Xiao[k], Jordi Sardans[f,g,], Yifei Zhang[a,b], Chuan Tong[a,b,***]**

[a]*Key Laboratory of Humid Subtropical Eco-geographical Process of Ministry of Education, Fujian Normal University, Fuzhou 350007, P.R. China*

[b]*School of Geographical Sciences, Fujian Normal University, Fuzhou 350007, P.R. China*

[c]*College of Environmental Science and Engineering, Fujian Normal University, Fuzhou 350007, P.R. China*

[d]*Collaborative Innovation Center of Atmospheric Environment and Equipment Technology, Jiangsu Key Laboratory of Atmospheric Environment Monitoring and Pollution Control (AEMPC), School of Environmental Science and Engineering, Nanjing University of Information Science and Technology, Nanjing 210044, China;*

[e]*Department of Geography and Environmental Science, University of Reading, Reading RG6 6AB, U.K.*

[f]*CSIC, Global Ecology Unit CREAF-CSIC-UAB, Bellaterra, Catalonia, Spain*

[g]*CREAF, Cderdanyola del Vallès, Catalonia, Spain*

[h]*Department of Biosciences, Swansea University, Swansea SA2 8PP, U. K.*

[i]*Department of Geography and Resource Management, The Chinese University of Hong Kong, Shatin, New Territories, Hong Kong SAR, China*

[j]*School of Geographical Sciences, East China Normal University, Shanghai 200241, China*

[k]*Key Laboratory of Watershed Geographic Sciences, Nanjing Institute of Geography and Limnology, Chinese Academy of Sciences, Nanjing, 210008, China*

***Correspondence to:** Derrick Y.F. Lai

Email: dyflai@cuhk.edu.hk

***Correspondence to:** Jordi Sardans

Email: j.sardans@creaf.uab.cat

****Correspondence to:** Chuan Tong

Email: tongch@fjnu.edu.cn

[1]Ping Yang, Jiafang Huang, and Hong Yang contributed equally to this work.

HIGHLIGHTS

- Aquaculture ponds emit CH_4
- Large variations in diffusive CH_4 fluxes are estimated by different thin boundary layer (TBL) models
- Methane fluxes measured by chambers and match those estimated by only some TBL models

A B S T R A C T

Static floating chambers (*FCs*) are the conventional method to measure CH_4 fluxes across the water-air interface in ponds, while thin boundary layer (*TBL*) modelling is increasingly used to estimate CH_4 fluxes. In this study, both *FCs* measurements and *TBL* models of gas transfer velocity were used to determine CH_4 evasion from aquaculture ponds in southeastern China. The surface water CH_4 concentrations ranged from 0.4 to 9.1 μmol L^{-1} with an average of 4.8±0.8 μmol L^{-1}. CH_4 flux was always positive, indicating the ponds as a persistent CH_4 source to air. Mean CH_4 flux based on different *TBL* models showed large variations, ranging between 19 and 316 μmol m^{-2} h^{-1}. Compared against the direct measurement *FCs*, three *TBL* models developed for the open sea, flowing estuarine system and lentic ecosystem (TBL_{W92a}, TBL_{RC01}, and TBL_{CL98}, respectively) overestimated CH_4 emission by 40-200%, while the wind tunnel-based *TBL* model (TBL_{LM86}) underestimated CH_4 emission. Two *TBL* models developed for lakes (TBL_{W92b} and TBL_{CW03}) gave estimates similar to *FCs*.

Keywords: Methane fluxes; Thin boundary layer models; Floating chambers; Water-air interface; Shallow aquaculture pond; Subtropical estuary

1. Introduction

Methane (CH_4) emissions from inland and coastal aquatic systems are potentially significant sources of atmospheric CH_4 (Bastviken et al., 2011; Musenze et al., 2014; Yang et al., 2011). CH_4 release from open water can be via diffusion and/or ebullition (bubbling) (Bastviken et al., 2004). Diffusive fluxes across the water-air interface are usually determined by using static floating chambers (*FCs*) or thin boundary layer (*TBL*) models. The *FCs* approach determines CH_4 fluxes based on the change in CH_4 concentrations in the chamber headspace over time. The *TBL* approach calculates the CH_4 flux from piston velocity and gas concentration in the water (Natchimuthu et al., 2017; Zhao et al., 2019). Previous studies have used either one of the two approaches to quantify CH_4 fluxes from aquatic ecosystems (e.g., Musenze et al., 2014; Natchimuthu et al., 2016; Wang et al., 2017; Welti et al., 2017). However, detailed comparison of the two methods is rare (e.g., Duchemin et al., 1999; Matthews et al., 2003), particularly for small pond ecosystems.

Recent studies have shown that very small ponds (area <0.001 km^2) are hotspots for CH_4 emission (Holgerson, 2015; Holgerson and Raymond, 2016; Wik et al., 2016; Yuan et al., 2019). However, the scalability of these measurements are largely constrained by the lack of rigorous quantifications of the area, number, and spatial distribution of small ponds globally (Jonsson et al., 2008; Zhao et al., 2019) and the different flux measurement methods between studies. In particular, the lack of consensus on gas flux measurement methods remains a major source of uncertainty in greenhouse gas assessment. For instance, the TBL_{LM86}, TBL_{Wan92a} and TBL_{Wan92b},

76 TBL_{RC01}, TBL_{CL98}, and TBL_{CW03} models, which were developed by Liss and Merlivatt
77 (1986), Wanninkhof (1992), Raymond and Cole (2001), Cole and Caraco (1998), and
78 Crusius and Wanninkhof (2003), respectively, are widely adopted wind-based models
79 to estimate CH_4 transfer velocities and fluxes. Among these *TBL* models, the
80 TBL_{LM86}, TBL_{Wan92a}, and TBL_{RC01} models were developed for wind tunnels, open sea,
81 and flowing estuarine systems, respectively, while TB_{Wan92b}, TBL_{CL98} and TBL_{CW03}
82 models were developed for the lentic ecosystem (e.g., lake). It is unclear to what
83 extent these different models are transferable to other aquatic ecosystems (Musenze et
84 al., 2014), and there is also a paucity of study comparing CH_4 fluxes by the different
85 approaches.

86 Aquaculture ponds are an important component of the global inland aquatic
87 habitats (FAO, 2017), and the total surface area of freshwater and brackish
88 aquaculture ponds is estimated to be around 110,000 km^2 (Verdegem and Bosma,
89 2009). Despite the importance of aquaculture ponds for CH_4 emission (Hu et al., 2016;
90 Wu et al., 2018; Yang et al., 2015, 2019a; Yuan et al., 2019), relevant CH_4 flux data
91 are disproportionately scarce, and the published results were predominantly
92 determined by *FCs* rather than *TBL* modelling (Hu et al., 2016; Wu et al., 2018; Yang
93 et al., 2015, 2019a). In this study, *FCs* and *TBL* models were used to compare CH_4
94 fluxes in aquaculture ponds in southeastern China. The aims were: (1) to evaluate the
95 performances of different wind-based *TBL* models for estimating CH_4 fluxes; (2) to
96 compare the diffusive CH_4 emissions from aquaculture ponds derived from *FCs*
97 measurements and *TBL* modellings; and (3) to assess which *TBL* model(s) can be used

to replace *FCs* for estimating CH_4 fluxes from ponds, with acceptable validity.

2. Materials and Methods

2.1. Study area

Our study sites are located at the central-western Shanyutan Wetlands in the Min River Estuary (MRE) in southeastern China (Figure S1, 26°00′36″–26°03′42″ N, 119°34′12″–119°40′40″ E). This area is characterized by a subtropical monsoon climate, with a multi-year annual average temperature and precipitation of 19.6 °C and 1,350 mm, respectively (Tong et al., 2010). The wetlands are dominated by a semidiurnal tide with a large tidal range (2.5-6 m) that follows a spring-neap-spring tidal cycle (Luo et al., 2014; Tong et al., 2010). The dominant vegetation are the native *Cyperus malaccensis* and *Phragmites australis*, and the invasive *Spartina alterniflora.* Over the past 10 years, much of area has been converted to aquacultural ponds (Yang et al., 2017a).

2.2. Aquaculture pond management

Small and shallow aquaculture earthen ponds (area of 0.8−2.5 ha and depth of 1.1−1.8 m) are a key feature in the MRE, covering a total area of around 234 ha in the Shanyutan Wetland (Yang et al., 2017b). Semi-intensive production is concentrated between June and November, which yields a single annual crop of shrimps. The ponds are filled with brackish water (average salinity of 2.0− 8.5‰) from the MRE. The shrimps are fed twice daily (at 07:00 and 16:00 hr) with commercial aquatic feed pellets containing 42% protein. Three to five paddlewheel aerators operate four times

a day (07:00–09:00, 12:00–14:00, 18:00–20:00, and 00:00–03:00 hr) to provide oxygen. For this study, three ponds separated by <10 m (see Table S1 for basic characteristics) (Zhang et al., 2019) were selected for the measurements. Additional details about the shrimp pond system and management can be found in Yang et al. (2017b).

2.3. Determination of dissolved CH_4 concentration

Field campaigns were carried out at the three ponds between June and November 2017 following the main aquaculture operation. In each pond, water and gas samples were collected at three sites along a foot-bridge that extended ~10 m from the embankment to the pond center. Samples were collected two or three times each month in each pond for a total of 15 times. The total number of samples was 3 ponds × 3 sites × 15 times = 135. To measure the dissolved CH_4 concentrations, surface water (at a depth of ~20 cm) was collected by a homemade water sampler and transferred into 55-mL gas-tight glass serum bottles that had been flushed with pond water 2-3 times. A 0.2 mL aliquot of saturated $HgCl_2$ solution was added to each bottle to inhibit bacterial activity of water sample (Borges et al., 2018; Hu et al., 2018), and the bottle was immediately sealed with a butyl rubber stopper and an aluminum screw cap to exclude air bubbles. Sample bottles were transported back to the laboratory in an ice-packed cooler. Dissolved CH_4 concentrations were measured within 2 d of collection using the headspace equilibration method: Approximately 25 mL of water in each bottle was displaced by N_2 gas (>99.999% purity) to create headspace. The bottle was then shaken vigorously for 20 min and left at room

temperature for 30 min to attain equilibrium between the air and the water phases (Cotovicz et al., 2016). Afterward, approximately 10 mL of the headspace was extracted and injected into a gas chromatograph (GC-2010, Shimadzu, Kyoto, Japan) equipped with a flame ionization detector (FID) to determine the CH_4 concentration. Standard CH_4 gas (at 2, 8, 500, 1000, and 10,000 ppm) was used to calibrate the FID. Dissolved CH_4 concentration was calculated based on the volume of water, headspace air and gas solubility coefficient for the specific water temperature and salinity (Farías et al., 2017; Wanninkhof, 1992; Xiao et al., 2017).

2.4. Determination of diffusive CH_4 flux across the water-air interface

2.4.1. Measurement using floating chambers

This study used a modified chamber placed on a floating buoy (Figure S2). The opaque floating chamber was made from inverted plastic basin (polyethylene/plexiglas®) with a volume and area of 5.2 L and 0.1 m^2, respectively. The chamber was covered with aluminum tape to minimize internal heating by sunlight (Natchimuthu et al., 2016; Yang et al., 2019). A thin gauze (pore diameter 0.001 mm) covering the opening minimized the entry of bubbles into the chamber (Figure S2). A fan inside the chamber mixed the headspace air during the sampling. In order to quantify the potential contribution of CH_4 ebullition flux from the ponds, total CH_4 fluxes were also determined using floating chamber without gauze.

The chamber was deployed for a period of 45 min and headspace air samples being extracted at 15-min intervals (0, 15, 30, 45 min) using 60-mL syringes equipped

with three-way stopcocks. The gas samples were immediately transferred into pre-evacuated airtight gas sampling bags (Dalian Delin Gas Packing Co., Ltd., China), transported to the laboratory, and analyzed within 48 h using a gas chromatograph (GC-2010, Shimadzu, Kyoto, Japan) equipped with a FID, following the method of Tong et al. (2010). The detection limit for CH_4 was 0.3 ppm, and the relative standard deviations of the measurements were ≤ 2.0% in 24 h.

CH_4 emission flux (F_{CH4}, μmol m^{-2} hr^{-1}) was calculated from the slope of the regression between headspace CH_4 concentration and time (Yang et al., 2019). Generally, if r^2 of the regression is > 0.90, the CH_4 emission is considered as diffusion only (Bastviken et al., 2010; Zhu et al., 2016). If r^2 is < 0.90, the emission is considered as a combination of ebullition and diffusion. The floating chambers with gauze (*FCs*-G) and without gauze (*FCs*-NG) showed distinctly linear (r^2>0.9) and nonlinear (r^2<0.9) increases in methane concentration, respectively; therefore, the contribution of ebullition could be calculated as the difference between the *FCs*-G and the *FCs*-NG measurements.

2.4.2. Estimation using thin boundary layer models

Saturation (*S*) of CH_4 in pond water was calculated as (Hu et al., 2018):

$$S = C_{water}/C_{Ws} = C_{water}/(\alpha \times C_{air}) \times 100\% \quad \text{(Eq. 1)}$$

where C_{water} is dissolved CH_4 concentration in pond water; C_{Ws} is the saturated CH_4 concentration (μmol L^{-1}); C_{air} is the atmospheric CH_4 concentration (μmol mol^{-1}) at the sampling site; and α is the Bunsen coefficient (Wanninkhof, 1992).

Diffusive flux of CH_4 (F, μmol m^{-2} hr^{-1}) across the water-air interface can be

described by a theoretical diffusion model (Musenze et al., 2014):

$$F = k \times (C_{water} - C_{eq}) \quad \text{(Eq. 2)}$$

where C_{water} (μmol L^{-1}) is the measured dissolved CH_4 concentration in surface water, C_{eq} (μmol L^{-1}) is the dissolved CH_4 concentration in equilibrium with the air above, and k is the gas transfer velocity (cm h^{-1}). The k value was parameterized as a function of wind speed and normalized for surface water temperature (T, ºC) using a Schmidt number (Sc) derived from Eq. 3 (Wanninkhof, 1992):

$$Sc = 2039.20 - 120.31T + 3.4209T^2 - 0.040437T^3 \quad \text{(Eq. 3)}$$

This study evaluated the variations in CH_4 fluxes estimated by eight widely used wind-based models developed for different environments, including wind tunnels, open sea, estuarine systems and lakes, as follows:

LM86 (Liss and Merlivatt 1986)

$$F_{LM86} = 0.17U_{10}(Sc/600)^{-2/3}(C_{water} - C_{eq}) \qquad 0 < U_{10} \leqq 3.6 \quad \text{(Eq. 4)}$$

$$F_{LM86} = (2.85U_{10} - 9.65)(Sc/600)^{-1/2}(C_{water} - C_{eq}) \qquad 3.6 < U_{10} \leqq 13 \quad \text{(Eq. 5)}$$

W92a (Wanninkhof, 1992)

$$F_{W92a} = 0.31U_{10}^2(Sc/660)^{-1/2}(C_{water} - C_{eq}) \quad \text{(Eq. 6)}$$

RC01 (Raymond and Cole, 2001)

$$F_{RC01} = 1.91exp(0.35U_{10})(Sc/600)^{-1/2}(C_{water} - C_{eq}) \quad \text{(Eq. 7)}$$

CL98 (Cole & Caraco, 1998)

$$F_{CL98} = [2.07 + (0.215 \times U_{10}^{1.7})](Sc/600)^{-2/3}(C_{water} - C_{eq}) \quad \text{(Eq. 8)}$$

W92b (Wanninkhof, 1992)

$$F_{W92b} = 0.45U_{10}^{1.64}(Sc/600)^{-1/2}(C_{water} - C_{eq}) \quad \text{(Eq. 9)}$$

CW03 (Crusius & Wanninkhof, 2003)

$$F_{CW03} = 0.72U_{10}(Sc/600)^{-2/3}(C_{water} - C_{eq}) \qquad U_{10} < 3.7 \quad \text{(Eq. 10)}$$

$$F_{CW03} = (4.33U_{10} - 13.3)(Sc/600)^{-1/2}(C_{water} - C_{eq}) \qquad U_{10} \geq 3.7 \quad \text{(Eq. 11)}$$

In the above equations, U_{10} was determined according to the logarithmic wind profile relationship (Crusius and Wanninkhof, 2003):

$$U_{10} = U_z[1 + \frac{(C_{d10})^{1/2}}{K}\ln(\frac{10}{z})] \quad \text{(Eq. 12)}$$

where U_z is the wind speed (m s^{-1}) at height z above the water surface (2.5 m in this study), C_{d10} is the drag coefficient at 10 m above the water surface (0.0013 m s^{-1}), and K is the von Karman constant (0.41). Generally, the calculation of U_{10} is sensitive ot the stability of the atmosphere. If the atmosphere over the aquatic systems is unstable, and the equation used to calculate U_{10} needs to be adjusted. The air-water temperature difference can be used to determine the atmospheric stability; if the air-water temperature difference is positive, the atmosphere is considered stable. During the study period, the air temperature was 0.1-3.8 ºC higher than water temperature, indicating that the atmosphere over the ponds was largely in the stability regime. Therefore, no adjustment was needed for U_{10}, and Eq. 12 was appropriate for calculating U_{10}. Some recent studies have applied surface renewal models that take

into account both wind speed and buoyancy to determine the k values (e.g., Czikowsky et al., 2018; MacIntyre et al., 2010; MacIntyre et al., 2018).

2.5. Measurement of meteorological and environmental variables

Meteorological variables including air temperature (A_T), air pressure (A_P) and precipitation were recorded using an automatic meteorological station (Vantage Pro 2, China) installed at the MRE weather station in the China Wetland Ecosystem Research Network. The distance between the automatic meteorological station and sampling ponds is about 75 m. The precision for air temperature, atmospheric pressure, and precipitation were ± 0.2 °C, ± 1.5 hPa, and ± 0.4 mm min^{-1}, respectively (Yang et al., 2020). Wind speed (W_S) was measured at 1 Hz at a resolution of 0.4 m s^{-1}.

Water temperature, electrical conductivity (EC), pH, dissolved oxygen (DO), total organic carbon (TOC) and total dissolved nitrogen (TDN) content of surface water (~20 cm below the water surface) were measured at each sampling site in all sampling campaigns. Water temperature and pH were measured by a portable pH/mV/Temperature meter (IQ150, IQ Scientific Instruments, USA), and EC and DO by an electrical conductivity meter (2265FS EC, Spectrum Technologies, USA) and a multiparameter water quality probe (550A YSI, USA), respectively. The relative standard deviations of EC, pH, and DO measurements were □1.0%, □1.0% and □2.0%, respectively.

Water samples for TOC and TDN analyses were collected using a 5-L plexiglass

water sampler, transferred to a 150-mL polyethylene bottle, and then transported to the laboratory in an ice-packed cooler. The water samples were filtered through a 0.45-μm cellulose acetate filter (Biotrans nylon membranes); the filtrates were then analysed by a TOC analyzer (TOC-$V_{CPH/CPN}$, Shimadzu, Kyoto, Japan) for TOC and a flow injection analyzer (Skalar Analytical SAN^{++}, The Netherlands) for NO_3^--N. The detection limits for NO_3^--N and TOC were 6 μg L^{-1} and 4 μg L^{-1}, respectively. The relative standard deviations of NO_3^--N and TOC measurements were □3.0% and □1.0%, respectively.

2.6. Statistical analysis

Repeated-measures analysis of variance (RM-ANOVA) was conducted to test the differences in diffusive CH_4 flux between the different approaches over the study period. Pearson correlation analysis was used to examine the relationships between (1) dissolved CH_4 concentration or CH_4 fluxes and environmental variables, and (2) diffusive CH_4 fluxes measured using *FCs* and those estimated using the *TBL* models. The coefficient of variation (CV) for CH_4 fluxes on each sampling campaign was determined by dividing the standard deviation by the mean value. Statistical analyses were conducted using the software SPSS (v. 17.0, SPSS Inc., USA) and the significance level was set at $p < 0.05$. Data are presented as mean ± 1 standard error.

Generalized linear modelling was conducted to compare the variables that influenced CH_4 emission flux from the different methods (i.e. *FCs* + 8 *TBL* models). The "gls" function from the "nlme" R package (Pinheiro et al., 2018) with a saturated

model was conducted for all variables (dissolved CH_4, U_{10}, water temperature, dissolved oxygen, total dissolved carbon and dissolved nitrate). This model was run using the stepAIC function in R "MASS" package that follows the Akaike Information Criterion (AIC) (Venables and Ripley, 2002). It was used to identify the best model (lowest AIC value) in each case.

3. Results

3.1. Meteorological and environmental variables

The average air temperature (A_T) and air pressure (A_P) during the study were 28.7±0.4 °C (range: 18.6−35.6 °C) and 1010.0±0.5 hPa (range: 985−1025 hPa), respectively. Notably, the maximal A_T appeared in July and the minimal A_P happened in August, different from the other months. W_S ranged from 0.2 to 18.8 m s^{-1}, and it varied between seasons, with a peak in July (Figure S3a). Approximately 92% of W_S fell within the range of 0.2−4.0 m s^{-1} (Figure S3b).

There were temporal variations in surface water characteristics during the study period. The mean water temperature ranged from 18.1 °C (November) to 34.4 °C (August) (Figure S4a), while the mean DO concentration varied between 9.4 mg L^{-1} (August) and 19.9 mg L^{-1} (November) (Figure S4). The mean TOC concentration varied between 9.9 mg L^{-1} (July) and 57.3 mg L^{-1} (November) (Figure S3), while NO_3^--N concentrations ranged from 504 µg N L^{-1} (June) to 10.7 µg N L^{-1} (November) (Figure S4).

3.2. Model estimated k values and dissolved CH_4 concentrations

286 The mean k value showed considerable variations between models: k_{RC01}
287 (6.5±0.8 cm h^{-1}) > k_{W92a} (3.5±0.7 cm h^{-1}) > k_{FCs} (3.2±0.4 cm h^{-1}) > k_{CL98} (2.9±0.3 cm
288 h^{-1}) > k_{CW03} (2.5±0.5 cm h^{-1}) > k_{W92b} (2.4±0.4 cm h^{-1}) > k_{LM86} (0.6±0.1 cm h^{-1}) (Figure
289 1).

290 Dissolved CH_4 concentration varied considerably during the study period
291 (0.1−31.1 µmol L^{-1}), with a large increase between June and August, followed by a
292 small decrease toward November (Figure 2). The water was supersaturated in CH_4 in
293 all ponds and on all sampling dates, with an overall mean of 4.8 ± 0.8 µmol L^{-1} (162.0
294 ±18.4 ppmv), equivalent to 8700% saturation (range of 200 – 5.9×10^4 % saturation).

295 *3.4. CH_4 flux estimates by using TBL models and FCs method*

296 There were considerable differences in the estimated diffusive CH_4 fluxes among
297 the *TBL* models (TBL_{RC01}: 215.9 ±39.2 µmol m^{-2} h^{-1}; TBL_{CL98}: 115.0 ±21.9 µmol m^{-2}
298 h^{-1}; TBL_{W92a}: 102.9 ±19.5 µmol m^{-2} h^{-1}; TBL_{W92b}: 78.3 ±13.9 µmol m^{-2} h^{-1}; TBL_{CW03}:
299 74.9 ±13.2 µmol m^{-2} h^{-1}; and, TBL_{LM86}: 19.5 ±3.7 µmol m^{-2} h^{-1}) (Table 1, Figure 3 and
300 Figure S5). Although there were marked variations in the flux estimates among the
301 various models, results from all models showed similar temporal patterns (Figure 3).
302 The largest fluxes were generally recorded between August and October, while the
303 lowest fluxes were consistently recorded in June and November (Figure 3).

304 Direct measurements using *FCs* with gauze (*FCs*-G) and without gauze
305 (*FCs*-NG) methods were 75.0 ±12.5 (Figure 3) and 2231.3 ±681.3 µmol m^{-2} h^{-1}
306 (Figure S6; Yang et al., unpublished data), showing significant difference between the

two methods (Independent Samples T-Test, F = 118.190, p<0.001). On average, ebullitive CH_4 flux accounted for 33%-99% of the total CH_4 emissions during the study period.

3.5. Environmental influences on dissolved CH_4 concentrations and fluxes

Pearson correlation analysis showed that dissolved CH_4 concentration was positively correlated with air temperature and TOC (p<0.01), and negatively with NO_3^--N and EC (p<0.01) (Table 2). CH_4 flux was positively correlated with air temperature (p<0.05), TOC and dissolved CH_4 concentration (p<0.01), and negatively with NO_3^--N (p<0.01) and EC (p<0.05) (Table 2 and Table S3). Environmental variables explained a larger proportion of variability in CH_4 flux derived from the *TBL* models (R^2=0.46-0.54) than those from direct *FCs* measurements (R^2=0.35) (Table S2).

4. Discussion

4.1. CH_4 supersaturation and degassing from aquaculture ponds

There are very few studies on CH_4 in small ponds, particularly, those created for aquaculture purposes. In this study, the dissolved CH_4 concentration in surface water of the aquaculture ponds ranged from 0.1 to 31.1 μmol L^{-1} during the study period, which was higher than that observed in many small ponds in Florida (~2.2 μmol L^{-1}; Barber et al., 1988), Colorado (~1.0 μmol L^{-1}; Bastviken et al., 2004), Wisconsin and Minnesota (0.3−2.3 μmol L^{-1}; Smith and Lewis, 1992) in the USA, in Sweden (~1.3 μmol L^{-1}; Natchimuthu et al., 2014), Canada (0.5−6.7 μmol L^{-1}; Pelletier et al., 2014),

and Siberia (~2.6 μmol L^{-1}; Repo et al., 2007). In addition, CH_4 concentration in our aquaculture ponds was generally larger than that in some nutrient-enriched rivers in China, i.e. Lixiahe River (0.2−0.8 μmol L^{-1}; Wu et al., 2019), Beitang Drainage River and Dagu Drainage River (0.3−1.7 μmol L^{-1}; Hu et al., 2018). Similar to other inland aquatic systems, such as lakes (e.g., Wen et al., 2016; Wik et al., 2016; Yan et al., 2018), reservoirs (e.g., Deemer et al., 2016; Musenze et al., 2014; Wang et al., 2017), rivers (e.g., Barbosa et al., 2016; Striegl et al., 2012), floodplains (Barbosa et al., 2020) and small ponds (e.g., Holgerson and Raymond, 2016; Wik et al., 2016), our aquaculture ponds were vastly supersaturated in CH_4 relative to air (2.71−599.81 times the equilibrium concentration) (Figure 2b). The small temperate ponds in the Yale Myers Forest in Connecticut, the USA, have some of the highest concentrations of CH_4 (21.0−58.9 μmol L^{-1}, equivalent to 119−2907 times the equilibrium concentration) (Holgerson, 2015). The CH_4 concentrations and supersaturation levels in our aquaculture ponds fall well within the range reported by Holgerson (2015), showing that aquaculture ponds in the subtropical estuaries are also hotspots for CH_4 production and emission.

In inland aquatic ecosystems, the strong CH_4 release is likely a result of large organic matter inputs from the catchment, algae and aquatic plants that sustain high methanogenesis rates (Finlay et al., 2009; Lundin et al., 2013; Venkiteswaran et al., 2013; Yan et al., 2018), as indicated by the significant relationship between dissolved CH_4 and nutrient level (Huttunen et al., 2003; Kortelainen et al., 2001; Wen et al., 2016). The shrimp ponds in this study are semi-artificial ecosystems that are

maintained through a daily feed supply for the production of aquatic animals. However, only a small portion of the feed input is converted into shrimp biomass, with the feed utilization efficiency of ~4.0−27.4% (Chen et al., 2016; Molnar et al., 2013; Yang et al., 2017b). Surface sediments in the aquaculture systems typically retain a large amount of organic matter from feces and residual feeds (Chen et al., 2016; Yang et al., 2017b) that can support high levels of CH_4 production and its subsequent release to atmosphere. Although organic matter content was not quantified in this study, our results confirmed the significantly correlation between dissolved CH_4 and TOC concentration (p<0.01; Table 2), which lends support to the notion that CH_4 supersaturation in the aquaculture ponds was related to the large input of organic matter.

4.2. Comparison of different TBL modelled CH_4 fluxes

Although previous studies have compared the performance of different *TBL* models in estimating diffusive CH_4 flux in inland waters (Amouroux et al., 2002; Li et al., 2015; Musenze et al., 2014; Xiao et al., 2017; Zappa et al., 2007), such comparison is scarce for shallow ponds, particularly aquaculture ponds. To the best of our knowledge, this study is the first attempt to compare the estimates of diffusive CH_4 flux using different *TBL* models over the whole aquaculture period in aquaculture ponds. Interestingly, although the patterns of temporal variations in diffusive CH_4 flux were largely consistent among the *TBL* models (Figure 3), there were clear differences in the magnitude of flux estimated from the different models (Table 1).

372 Notably, the mean flux estimated by the TBL_{RC01} model (215.6 μmol m^{-2} h^{-1}) was
373 an order of magnitude greater than that derived from the TBL_{LM86} model (19.4 μmol
374 m^{-2} h^{-1}, Figure 3). Moreover, CH_4 flux estimated by the TBL_{RC01} model was 2 - 3
375 times larger than that by the TBL_{W92a}, TBL_{CL98}, TBL_{W92b} and TBL_{CW03} models (Table 1
376 and Figure S5). However, there was no significant difference between the TBL_{W92a}
377 and TBL_{CL98} models (p>0.05; Table 1 and Figure S5) or between the TBL_{W92b} and
378 TBL_{CW03} models (p>0.05; Table 1 and Figure S5). In other inland waters (river and
379 reservoirs), Gao et al. (2014) and Musenze et al. (2014) also found that the estimated
380 diffusive CH_4 fluxes derived from the TBL_{RC01} model were substantially greater than
381 those from other *TBL* models.

382 The differences in the estimated CH_4 flux between different *TBL* models were
383 likely a result of different weighting of wind as a driver of gas transfer velocity
384 (Musenze et al., 2014, Figure 1). Because these wind-based models were originally
385 developed for specific environments under different conditions (Gao et al., 2014;
386 Musenze et al., 2014), their suitability for other situations could be questioned (Bade,
387 2009; Musenze et al., 2014; Schilder et al., 2013). The TBL_{CL98} and TBL_{CW03} models
388 were developed for lentic ecosystems under a range of wind speed, which most
389 closely resemble aquaculture pond conditions. One may therefore argue that these two
390 models would be most applicable to aquaculture ponds, although more *in situ*
391 measurement will be needed to further increase the accuracy of the estimate.

392 *4.3. Comparison of CH_4 fluxes derived from FCs measurement and TBL models*

393 Previous studies have shown that CH_4 fluxes estimated by *TBL* models tend to be

394 lower than those measured by *FCs* (Chuang et al., 2017; Duchemin et al., 1999; Li et
395 al., 2015; Matthews et al., 2003). This study also compared CH_4 fluxes measured by
396 *FCs* and those estimated by *TBL* models over the aquaculture season (Table 1 and
397 Figure S5). Although there were significant correlations between *TBL* model estimates
398 and *FCs* measurements ($p < 0.05$ in all cases), the agreement between the two
399 methods varied considerably between models (Figure 4). The TBL_{W92b} and TBL_{CW03}
400 models gave the largest r^2 values (0.82 and 0.83, respectively) and good agreements
401 with *FCs* measurements (slope = 0.92 and 0.89, respectively), whereas TBL_{CL98}
402 yielded mean estimates virtually identical to *FCs* measurements (slope = 1) but with
403 larger variability around the mean ($r^2 = 0.53$) (Figures 4d-f). In contrast, TBL_{LM86}
404 vastly underestimated FCs fluxes whereas TBL_{RC01} grossly overestimated FCs fluxes
405 (Figures 4a,b). Approximately 80% of the diffusive CH_4 fluxes estimated by the
406 models fell within the range measured by the *FC* method.

407 Balancing the consideration of overall agreement (regression slope) and estimate
408 variability (regression r^2), the TBL_{W92b} and TBL_{CW03} models appeared to give the best
409 approximations of *FCs* measurements. While previous studies showed that *FCs* were
410 more appropriate for determining greenhouse gas fluxes in heterogeneous
411 environments such as lakes and reservoirs (Cole et al., 2010; Duchemin et al., 1999;
412 Murray et al., 2015; Vachon et al., 2010; Wu et al., 2018), our results suggest that
413 TBL_{W92b} and TBL_{CW03} models are reliable alternatives for estimating CH_4 diffusive
414 flux in shallow aquaculture ponds.

415 In addition to diffusive flux from the water column, bottom sediment could also

416 contribute to CH_4 emission via ebullition, especially in eutrophic, shallow aquaculture
417 ponds. This is illustrated by the differences in the measured CH_4 flux using *FCs* with
418 and without gauze in our aquaculture ponds (Figure S6). The CH_4 flux measured by
419 *FCs* without gauze (2231.3 ±681.3 μmol m^{-2} h^{-1}) were one to two orders of magnitude
420 higher than that by *FCs* with gauze (75.0 ±12.5 μmol m^{-2} h^{-1}) (Figure S6); from this
421 ebullition was estimate to contribute 96.6% to the total CH_4 emissions. Overall, our
422 results showed that ebullition was the primary path of CH_4 emission in aquaculture
423 ponds, and that ebullitive flux vs. diffusive flux could be easily resolved with a simple
424 design of *FCs* with a detachable gauze.

425 *4.4. Implications of the comparison between different methods*

426 The *FCs* method is the popular technique for measuring CH_4 emissions due to its
427 ability to detect low fluxes and the simplicity of its operating principle (Bastviken et
428 al., 2015; Lorke et al., 2015; Musenze et al., 2014; Podgrajsek et al., 2014). However,
429 the *FCs* method requires time-consuming manual operation, which limits the
430 frequency of measurements and can be difficult to deploy in remote areas (Acosta et
431 al., 2017; Morin et al., 2017). Improvement of the global CH_4 budget would require
432 high-resolution emission data covering large time and spatial scales, which obviously
433 is difficult to achieve with the *FCs* method.

434 Large-scale estimates of aquatic CH_4 emissions using *TBL* models has been
435 gaining popularity (Holgerson and Raymond, 2016; Martinez-Cruz et al., 2016;
436 Musenze et al., 2014; Wang et al., 2017) due to their simplicity, practicality and low
437 cost. There are, however, different *TBL* models to choose from, and the large

differences in the model performances (Figure 4) mean that selecting the appropriate model(s) would be critical, or otherwise large errors would occur when upscaling the results from small ponds to the regional/ global scale. Our results suggest that TBL_{W92b} and TBL_{CW03} models could be used as effective and convenient alternatives to *FCs* in shallow aquaculture ponds.

4.5. Limitation and future research

The *FCs* method is a common method to measure CH_4 fluxes from aquatic ecosystems. However, *FCs* may create microenvironments that affect the boundary layer conditions through, for instance, blockage of wind, change of atmospheric pressure at the measurement point, and change in the gas transfer rate through pressure build-up (Duchemin et al., 1999; Matthews et al., 2003; Musenze et al., 2014). For example, the turbulence resulted from the chamber walls can enhance the efficiency of gas exchange and increase gas fluxes during low wind conditions (Matthews et al., 2003; Xiao et al., 2016).

TBL models rely on the gas transfer velocity coefficient (k_x), which itself is estimated from some empirical wind-based models. Effects of artificial aeration, which is commonly done in aquaculture ponds, on k_x are unknown. More importantly, the *TBL* models ignore the effect of buoyancy fluxes near the air-water interface on k_x. An alternative is the surface renewal model (SRM), which considers both wind speed and buoyancy (e.g., Czikowsky et al., 2018; MacIntyre et al., 2010; MacIntyre et al., 2018).

The use of eddy covariance (EC) technique is increasingly popular as it can

provide a better characterization of the variation in CH_4 fluxes through quasi-continuous measurements (Acosta et al., 2017; Morin et al., 2017; Xiao et al., 2014; Zhao et al., 2019). However, its application in small water bodies (e.g., ponds) is limited by footprint contamination (Zhao et al., 2019). Developing a practical and effective way to reduce the flux footprint and the contamination from gaseous sources outside the water body will allow broader application of EC method in the future.

Different methods have their own limitations; careful comparison and cross calibration would be needed to increase the overall accuracy of these methods and to improve the global CH_4 budget.

5. Conclusions

Despite the large CH_4 emission potential from small ponds, there are few studies comparing the different methods to estimate CH_4 fluxes across the water-air interface. In this study, *FCs* and *TBL* models were used to estimate CH_4 fluxes from aquaculture ponds. Our results indicate that dissolved CH_4 concentrations in the subtropical shallow aquaculture ponds were on average ~87 times oversaturated relative to the ambient air, and thus the ponds acted as strong atmospheric CH_4 sources. The high organic matter loading contributed to CH_4 supersaturation in the ponds. This study for the first time compared the CH_4 fluxes measured directly by floating chambers (*FCs*) and those estimated by thin boundary layer (*TBL*) models (TBL_{LM86}, TBL_{W92a}, TBL_{RC01}, TBL_{CL98}, TBL_{W92b}, and TBL_{CW03}). The model estimates of diffusive CH_4 fluxes were highly variable, and were overall 27 - 300% larger than those measured by *FCs*. The TBL_{W92b} and TBL_{CW03} models provided a robust and simple alternative to *FCs* in

estimating diffusive CH_4 fluxes. Our results suggest that the comparison of different methods and selection of the most appropriate method(s) should be a high research priority to improve the accuracy of greenhouse gas fluxes from aquaculture ponds and other aquatic ecosystems.

Declaration of competing interest

The authors declare that they have no known competing financial interests or personal relationships that could have appeared to influence the work reported in this paper.

Acknowledgments

This research was financially supported by the National Science Foundation of China (grant numbers 41801070 and 41671088), National Key Research & Development Plan "Strategic International Scientific and Technological Innovation Cooperation" (2016YFE0202100), Council of the Hong Kong Special Administrative Region, China (CUHK458913 and CUHK Direct Grant SS15481), Spanish Government (grant CGL2016-79835), Catalan Government (grant SGR 2017-1005), European Research Council (Synergy grant ERC-SyG-2013-610028), Open Research Fund Program of Jiangsu Key Laboratory of Atmospheric Environment Monitoring & Pollution Control (grant KHK1806), Priority Academic Program Development of Jiangsu Higher Education Institutions (PAPD), and Minjiang Scholar Programme. We thank Qianqian Guo, Guanghui Zhao, and Ling Li of the School of Geographical Sciences, Fujian Normal University, for assistance in the field.

References

Acosta, M., Dušek, J., Chamizo, S., Serrano-Ortiz, P., Pavelka, M., 2019. Autumnal fluxes of CH_4 and CO_2 from Mediterranean reed wetland based on eddy covariance and chamber methods. Catena 183, 104191. https://doi.org/10.1016/j.catena.2019.104191

Amouroux, D., Roberts, G., Rapsomanikis, S., Andreae, M.O., 2002. Biogenic gas (CH_4, N_2O, DMS) emission to the atmosphere from near-shore and shelf waters of the north-western Black Sea. Estuar. Coast. Shelf S. 54(3), 575-587.https://doi.org/10.1006/ecss.2000.0666

Bade, D.L., 2009. Gas Exchange at the Air-Water Interface. InEncyclopedia of Inland Waters; Likens, G. E., Ed.; Academic Press:Oxford, pp 70-78.

Barber, T.R., Burke, R.A. Jr., Sackett, W.M., 1988. Diffusive flux of methane from warm wetlands. Global Biogeochem. Cy. 2, 411-425.

Barbosa, P.M., Melack, J.M., Amaral, J.H.F., Scofield, V., Farjalla V., Forsberg, B.R., 2016. Diffusive methane fluxes from Negro, Solimões and Madeira rivers and fringing lakes in the Amazon basin. Limnol. Oceanogr. 61, S221-237. https://doi.org/10.1002/lno.10358

Barbosa, P.M., Melack, J.M., Amaral, J.H.F., MacIntyre, S., Kasper, D., Cortes, A.C., Farjalla, V.F., Forsberg, B.R., 2020. Dissolved methane concentrations and fluxes to the atmosphere from a tropical floodplain lake. Biogeochemistry 148, 129-151. https://doi.org/10.1007/s10533-020-00650-1

Bastviken, D., Cole, J., Pace, M., Tranvik, L., 2004. Methane emissions from lakes: Dependence of lake characteristics, two regional assessments, and a global estimate. Global Biogeochem. Cy. 18, GB4009. https://doi.org/10.1029/2004GB002238

Bastviken, D., Santoro, A.L., Marotta, H., Pinho, L.Q., Calheiros, D.F., Crill, P., Enrich-Prast, A., 2010. Methane emissions from Pantanal, South America, during the low water season: Toward more comprehensive sampling. Environ. Sci. Technol. 44,5450-5455.

Bastviken, D., Tranvik, L.J., Downing, J.A., Crill, P.M., Enrich-Prast, A., 2011. Freshwater methane emissions offset the continental carbon sink. Science 331, 50.

Bastviken, D., Sundgren, I., Natchimuthu, S., Reyier, H., Gålfalk, M., 2015. Cost-efficient approaches to measure carbon dioxide (CO_2) fluxes and concentrations in terrestrial and aquatic environments using mini loggers. Biogeosciences 12(12), 3849-3859. https://doi.org/10.5194/bg-12-3849-2015

Borges, A.V., Speeckaert, G., Champenois, W., Scranton, M.I., Gypens, N., 2018. Productivity and temperature as drivers of seasonal and spatial variations of dissolved methane in the Southern

534 Bight of the North Sea. Ecosystems 21(4), 583-599.
535 https://doi.org/10.1007/s10021-017-0171-7
536 Chen, Y., Dong, S.L., Wang, F., Gao, Q.F., Tian, X.L., 2016. Carbon dioxide and methane fluxes
537 from feeding and no-feeding mariculture ponds. Environ. Pollut. 212,
538 489-497.http://dx.doi.org/10.1016/j.envpol.2016.02.039
539 Chuang, P.-C., Young, M.B., Dale, A.W., Miller, L.G., Herrera-Silveira, J.A., Paytan, A., 2017.
540 Methane fluxes from tropical coastal lagoons surrounded by mangroves, Yucatán, Mexico. J.
541 Geophys. Res. Biogeosci., 122(5), 1156-1174. https://doi.org/10.1002/2017JG003761
542 Cole, J.J., Caraco, N.F., 1998. Atmospheric exchange of carbon dioxide in a low-wind oligotrophic
543 lake measured by the addition of SF6. Limnol. Oceanogr. 43(4): 647-656.
544 Cole, J.J., Bade, D.L., Bastviken, D., Pace, M.L., Van de Bogert, M., 2010. Multiple approaches to
545 estimating air-water gas exchange in small lakes. Limnol. Oceanogr. Methods 8,
546 285-293.https://doi.org/10.4319/lom.2010.8.285
547 Cotovicz Jr., L.C., Knoppers,B.A., Brandini,N., Poirier,D., Costa Santos,S.J., Abril, G., 2016.
548 Spatio-temporal variability of methane (CH_4) concentrations and diffusive fluxes from a
549 tropical coastal embayment surrounded by a large urban area (Guanabara Bay, Rio de Janeiro,
550 Brazil). Limnol. Oceanogr.61(S1), 238-252. https://doi.org/10.1002/lno.10298
551 Crusius, J., Wanninkhof, R., 2003. Gas transfer velocities measured at low wind speed over a lake.
552 Limnol. Oceanogr. 48(3), 1010-1017.
553 Czikowsky, M.J., MacIntyre, S., Tedford, E.W., Vidal, J., Miller, S.D., 2018. Effects of wind and
554 buoyancy on carbon dioxide distribution and air-water flux of a stratified temperate lake. J.
555 Geophys. Res.-Biogeo. 123, 2305-2322. https://doi.org/10.1029/2017JG004209
556 Deemer, B.R., Harrison, J.A., Li, S.Y., Beaulieu, J.J., Delsontro, T., Barros, N., Bezerra-Neto, J.F.,
557 Powers, S.M., dosSantos, M.A., Vonk, J.A., 2016. Greenhouse gas emissions from reservoir
558 water surfaces: A New Global Synthesis. Bioscience 66(11), 949-964.
559 https://doi.org/10.1093/biosci/biw117
560 Descloux, S., Chanudet, V., Serça,D., Guérin, F., 2017. Methane and nitrous oxide annual
561 emissions from an old eutrophic temperate reservoir. Sci. Total Environ. 598,
562 959-972.http://dx.doi.org/10.1016/j.scitotenv.2017.04.066

563 Duchemin, E., Lucotte, M., Canuel, R., 1999. Comparison of static chamber and thinboundary
564 layer equation methods for measuring greenhouse gas emissionsfrom large water bodies.
565 Environ. Sci. Technol. 33, 350-357. http://dx.doi.org/10.1021/es9800840
566 FAO, 2017. Fishery and aquaculture statistics (global aquaculture production 1950-2014).
567 FishStatJ. http://www.fao.org/fishery/statistics/software/fishstatj/en.
568 Farías, L., Sanzana, K., Sanhueza-Guevara, S., Yevenes, M.A., 2017. Dissolved methane
569 distribution in the Reloncaví Fjord and adjacent marine system during austral winter (41°-43°
570 S). Estuar. Coast. 40(6), 1592-1606. https://doi.org/10.1007/s12237-017-0241-2
571 Finlay, K., Leavitt, P.R., Wissel, B., Prairie, Y.T., 2009. Regulation of spatial andtemporal
572 variability of carbon flux in six hard-water lakes of the Northern GreatPlains. Limnol.
573 Oceanogr. 54, 2553-2564. https://doi.org/10.4319/lo.2009.54.6
574 Gålfalk, M., Bastviken, D., Fredriksson, S., Arneborg, L., 2013. Determination of the piston
575 velocity for water-air interfaces using flux chambers, acoustic Doppler velocimetry, and IR
576 imaging of the water surface. J. Geophys. Res. Biogeosci. 118, 770-782.
577 https://doi.org/10.1002/jgrg.20064
578 Gao, J., Zheng, X.H., Wang, R., Liao, T.T., Zuo, J.W., 2014. Preliminary comparison of the static
579 floating chamber and thediffusion model methods for measuring water−atmosphere exchanges
580 of methane and nitrous oxide from inland water bodies. ClimaticEnviron. Res. 19(3), 290-302.
581 (In Chinese)
582 Hirota, M., Senga, Y., Seike, Y., Nohara, S., Kunii, H., 2007. Fluxes of carbon dioxide, methane
583 and nitrous oxide in two contrastive fringing zones of coastal lagoon, Lake Nakaumi, Japan.
584 Chemosphere, 68(3), 597-603. https://doi.org/10.1016/j.chemosphere.2007.01.002
585 Hu, B.B., Wang, D.Q., Zhou, J., Meng, W.Q., Li, C.W., Sun,Z.B., Guo, X., Wang, Z.L., 2018.
586 Greenhouse gases emission from the sewage draining rivers. Sci. Total Environ. 612,
587 1454-1462. http://dx.doi.org/10.1016/j.scitotenv.2017.08.055
588 Holgerson, M.A., 2015. Drivers of carbon dioxide and methane supersaturation in small,
589 temporary ponds. Biogeochemistry 124(1-3), 305-318.
590 https://doi.org/10.1007/s10533-015-0099-y
591 Holgerson, M.A., Raymond, P. A., 2016. Large contribution to inland water CO_2 and CH_4
592 emissions from very small ponds. Nat. Geosci. 9(3): 222-226.
593 https://doi.org/10.1038/NGEO2654

Hu, Z.Q., Wu, S., Ji, C., Zou, J.W., Zhou, Q.S., Liu, S.W., 2016. A comparison of methane emissions following rice paddies conversion to crab-fish farming wetlands in southeast China. Environ. Sci. Pollut. Res. 23(2),1505-1515. https://doi.org/0.1007/s11356-015-5383-9

Huttunen, J.T., Alm, J., Liikanen, A., Juutinen, S., Larmola, T., Hammar, T., et al., 2003. Fluxes of methane, carbon dioxide and nitrous oxide in boreal lakes and potential anthropogenic effects on the aquaticgreenhouse gas emissions. Chemosphere 52, 609-621.https://doi.org/10.1016/S0045-6535(03)00243-1

IPCC, 2019. In: Calvo Buendia, E., Tanabe, K., Kranjc, A., Baasansuren, J., Fukuda, M., Ngarize, S. (Eds.), 2019 Refinement to the 2006 IPCC Guidelines for National Greenhouse Gas Inventories, Volum 4. IPCC, Switzerland. Kanagawa, Japan Chapter 07.

Jonsson, A., Åberg, J., Lindroth, A., Jansson, M., 2008. Gas transfer rate and CO_2 fluxbetween an unproductive lake and the atmosphere in northern Sweden. J. Geophys.Res. 113, G04006.

Kortelainen, P., Huttunen, J.T., Vaisanen, T., Mattsson, T., Karjalainen, P.,Martikainen, P.J., 2001. CH_4, CO_2 and N_2O supersaturation in 12 Finnish lakesbefore and after ice-melt. In: Williams, W.D. (Ed.), International Association ofTheoretical and Applied Limnology, vol. 27, pp. 1410-1414. Pt 3, Proceedings. 27.

Li, J.H., Pu, J.B., Sun, P.A., Yuan, D.X., Liu, W., Zhang, T., Mo, X., 2015. Summer greenhouse gases exchange flux across water-air interface in three water reservoirs located in different geologic setting in Guangxi, China. Environ. Sci. 36(11), 4032-4042. (In Chinese)

Liss, P.S., Merlivat, L.,1986. Air-Sea gas exchange rates: introduction and synthesis. In The Role of Air-Sea Exchange in Geochemical Cycling. In: Buat-Menard P, (eds.). Reidel: Dordrecht, The Netherlands, pp,´113-129.

Liu, S.W., Hu, Z.Q., Wu, S., Li, S.Q., Li, Z.F., Zou, J.W., 2015. Methane and nitrous oxide emissions reduced following conversion of rice paddies to inland crab-fish aquaculture in southeast China. Environ. Sci. Technol. 50(2), 633-642.https://doi.org/10.1021/acs.est.5b04343

Lorke, A., Bodmer, P., Noss, C., Alshboul, Z., Koschorreck, M., Somlai-Haase, C., Bastviken, D., Flury, S., McGinnis, D.F., Maeck, A., Müller, D., Premke, K., 2015. Technical note: Drifting versus anchored flux chambers for measuring greenhouse gas emissions from running waters. Biogeosciences 12(23), 7013-7024. http://dx.doi.org/10.5194/bg-12-7013-2015.

624 Lundin, E.J., Giesler, R., Persson, A., Thompson, M.S., Karlsson, J., 2013. Integrating carbon
625 emissions from lakes and streams in a subarcticcatchment. J. Geophys. Res.-Biogeo. 118,
626 1200–1207. https://doi.org/10.1002/jgrg.20092
627 Luo, M., Zeng, C.S., Tong, C., Huang, J.F., Yu, Q., Guo, Y.B., Wang, S.H., 2014. Abundance
628 andspeciation of iron across a subtropical tidal marsh of the Min River estuary in the eastChina
629 Sea. Appl. Geochem. 45, 1-13.
630 MacIntyre, S., Crowe, A.T., Cortés, A., Arneborg, L., 2018. Turbulence in a small arctic pond.
631 Limnol. Oceanogr. 63, 2337-2358. http://dx.doi.org/10.1002/lno.10941
632 MacIntyre, S., Jonsson, A.J., Jansson, M., Aberg, J., Turney, D., Miller, S., 2010. Buoyancy flux,
633 turbulence, and the gas transfer coefficient in a stratified lake. Geophys. Res. Lett. 37.
634 http://dx.doi.org/10.1029/2010GL044164
635 Matthews, C.J.D., St. Louis, V.L., Hesslein, R.H., 2003. Comparison of three techniques used to
636 measure diffusive gas exchange from sheltered aquatic surfaces. Environ. Sci. Technol. 37(4),
637 772-780.https://doi.org/10.1021/es0205838
638 Morin, T.H., Bohrer, G., Stefanik, K.C., Rey-Sanchez, A.C., Matheny, A.M. and Mitsch, W.J.,
639 2017. Combining eddy-covariance and chamber measurements to determine the methane
640 budget from a small, heterogeneous urban floodplain wetland park. Agr. Forest Meteorol. 237,
641 160-170. http://dx.doi.org/10.1016/j.agrformet.2017.01.022
642 Molnar, N., Welsh, D. T., Marchand, C., Deborde, J., Meziane, T., 2013. Impacts of shrimp farm
643 effluent on water quality, benthic metabolism and N-dynamics in a mangrove forest (New
644 Caledonia). Estuar. Coast. Shelf S. 117, 12-21. https://doi.org/10.1016/j.ecss.2012.07.012
645 Murray, R.H., Erler, D.V., Eyre, B.D., 2015. Nitrous oxidefluxes in estuarine environments:
646 response to global change.Global Change Biol. 21(9), 3219-3245.
647 https://doi.org/10.1111/gcb.12923.
648 Musenze, R. S., Grinham, A., Werner, U., Gale, D., Sturm, K., Udy, J., Yuan, Z.G., 2014.
649 Assessing the spatial and temporal variability of diffusive methane and nitrous oxide
650 emissions from subtropical freshwater reservoirs. Environ. Sci. Technol. 48, 14499-14507.
651 https://doi.org/10.1021/es505324h
652 Natchimuthu, S., Selvam, B.P., Bastviken, D., 2014. Influence of weather variables on methane
653 and carbon dioxide flux from a shallowpond. Biogeochemistry, 119(1-3), 403-413.
654 https://doi.org/10.1007/s10533-014-9976-z

Natchimuthu, S., Sundgren, I., Gålfalk, M., Klemedtsson, L., Crill, P., Danielsson, Å., Bastviken, D., 2016. Spatio-temporal variability of lake CH_4 fluxes and its influence on annual whole lake emission estimates. Limnol. Oceanogr. 61(S1), S13-S26.https://doi.org/10.1002/lno.10222

Natchimuthu, S., Sundgren, I., Gålfalk, M., Klemedtsson, L., Bastviken, D., 2017. Spatiotemporal variability of lake pCO_2 and CO_2 fluxes in a hemiboreal catchment. J. Geophys. Res. Biogeosci. 122, 30-49. https://doi.org/10.1002/2016JG003449

Repo, M.E., Huttunen, J.T., Naumov, A.V., Chichulin, A.V., Lapshina, E.D., Bleuten, W., Martikainen, P.J., 2007. Release of CO_2 and CH_4 from small wetland lakes in western Siberia. Tellus B 59, 788-796.

Pelletier, L., Strachan, I.B., Garneau, M., Roulet, N.T., 2014. Carbon release from boreal peatland open water pools: Implication for the contemporary C exchange. J. Geophys. Res.-Biogeo. 119, JG002423.

Pinheiro, J. et al. nlme: linear and nonlinear mixed effects models.-R package ver. 3.1-137. (2018).

Podgrajsek, E., Sahlee, E., Bastviken, D., Holst, J., Lindroth, A., Tranvik, L., Rutgersson, A., 2014. Comparison of floating chamber and eddy covariance measurements of lake greenhouse gas fluxes. Biogeosciences 11(15), 4225-4233. https://doi.org/10.5194/bg-11-4225-2014

Raymond, P., Cole, J., 2001. Gas exchange in rivers and estuaries: Choosing a gas transfer velocity. Estuar. Coast. 24(2), 312-317.

Schilder, J., Bastviken, D., van Hardenbroek, M., Kankaala, P., Rinta, P., Sto¨tter, T., Heiri, O., 2013. Spatial heterogeneity and lakemorphology affect diffusive greenhouse gas emission estimates oflakes. Geophys. Res. Lett. 40(21), 5752-5756.https://doi.org/10.1002/2013GL057669

Schubert, C.J., Diem, T., Eugster, W., 2012. Methane emissions from a small wind shielded lake determined by eddy covariance, flux chambers, anchored funnels, and boundary model calculations: a comparison. Environ. Sci. Technol. 46(8), 4515-4522. https://doi.org/10.1021/es203465x

Smith, L.K., Lewis, W.M.Jr., 1992. Seasonality of methane emissions from five lakes and associated wetlands of the Colorado Rockies. Global Biogeochem. Cy. 6,323-338.

Striegl, R.G., Dornblaser, M.M., McDonald, C.P., Rover, J.R., Stets, E.G., 2012. Carbon dioxide and methane emissions from the YukonRiver system. Global Biogeochem. Cy. 26, GB0E05. https://doi.org/10.1029/2012GB004306

686 Tangen, B.A., Finocchiaro, R.G., Gleason, R.A., Dahl, C.F., 2016. Greenhouse gas fluxes of a
687 shallow lake in south-central NorthDakota, USA. Wetlands36(4), 779-787.
688 https://doi.org/10.1007/s13157-016-0782-3
689 Tong, C., Wang, W.Q., Zeng, C.S., Marrs, R., 2010. Methane emissions from a tidal marsh in the
690 Min River estuary, southeast China. J. Environ. Sci. Heal. A. 45,
691 506-516.https://doi.org/10.1080/10934520903542261
692 Vachon, D., Prairie, Y.T., Cole, J.J., 2010. The relationship between near-surface turbulence and
693 gas transfer velocity in freshwatersystems and its implications for floating chamber
694 measuiements of gas exchange. Limnol. Oceanogr. 55(4), 1723-1732.
695 https://doi.org/10.4319/lo.2010.55.4.1723
696 Venables, W.N., Ripley, B.D., 2002. Modern and Applied Statistics with S. Fourth edition.
697 Springer, New York. https://www.stats.ox.ac.uk/pub/MASS4
698 Venkiteswaran, J.J., Schiff, S.L., St. Louis, V.L., Matthews, C.J.D., Boudreau, N.M., Joyce, E.M.,
699 Beaty, K.G., Bodaly, R.A., 2013. Processes affecting greenhouse gas production in
700 experimental borealreservoirs. Global Biogeochem. Cy. 27(2),
701 567-577.https://doi.org/10.1002/gbc.20046
702 Verdegem, M.C.J., Bosma, R.H., 2009.Water withdrawal forbrackish and inland aquaculture, and
703 options to producemore fish in ponds with present water use. Water Policy11 (Suppl 1), 52-68.
704 Wang, X.F., He, Y.X., Yuan, X.Z., Chen, H., Peng,C.H., Yue, J.S., Zhang, Q.Y., Diao, Y.B., Liu,
705 S.S., 2017. Greenhouse gases concentrations and fluxes from subtropical small reservoirs in
706 relation with watershed urbanization. Atmos. Environ. 154, 225-235.
707 https://doi.org/10.1016/j.atmosenv.2017.01.047
708 Wanninkhof, R., 1992. Relationship between wind speed and gas exchange over the ocean. J.
709 Geophys. Res. Oceans 97(C5), 7373-7382. https://doi.org/10.1029/92JC00188
710 Welti, N., Hayes, M., Lockington, D., 2017. Seasonal nitrous oxide and methane emissions across
711 a subtropical estuarine salinity gradient. Biogeochemistry 132,
712 55-69.https://doi.org/10.1007/s10533-016-0287-4
713 Wen, Z.D., Song, K.S.,, Zhao, Y., Jin, X.L., 2016. Carbon dioxide and methane supersaturation in
714 lakes of semi-humid/semi-arid region, Northeastern China. Atmos. Environ. 138: 65-73.
715 http://dx.doi.org/10.1016/j.atmosenv.2016.05.009
716 Wik, M., Varner, R.K., Anthony, K.W., MacIntyre, S., Bastviken, D., 2016. Climate-sensitive

northern lakes and ponds are critical components of methane release. Nat. Geosci. 9(2), 99.

World Meteorological Organization, 2017. WMO Greenhouse Gas Bulletin No.13 (October 2017). https://library.wmo.int/opac/doc_num.php?explnum_id=3084.pdf.

Wu, S., Hu, Z.Q., Hu, T., Chen, J., Yu, K., Zou, J.W., Liu, S.W., 2018. Annual methane and nitrous oxide emissions from rice paddies and inland fish aquaculture wetlands in southeast China. Atmos. Environ. 175, 135-144.https://doi.org/10.1016/j.atmosenv.2017.12.008

Wu, S., Li, S.Q., Zou, Z.H., Hu, T., Hu, Z.Q., Liu , S.W., Zou, J.W., 2019. High methane emissions largely attributed to ebullitive fluxes from a subtropical river draining a rice paddy watershed in China. Environ. Sci. Technol. 53, 349-3507. https://doi.org/10.1021/acs.est.8b05286

Xiao, S.B., Wang, C.H., Wilkinson, R.J., Liu,D.F., Zhang, C., Xu,W.N., Yang, Z.J., Wang, Y.C., Lei, D., 2016. Theoretical model for diffusive greenhouse gas fluxes estimation across water-air interfaces measured with the static floating chamber method. Atmos. Environ. 137, 45-52. http://dx.doi.org/10.1016/j.atmosenv.2016.04.036

Xiao, Q.T., Zhang, M., Hu, Z.H., Gao, Y.Q., Hu, C., Liu, C., Liu, S.D., Zhang, Z., Zhao, J.Y., Xiao, W., Lee, X., 2017. Spatial variations of methane emission in a large shallow eutrophic lake in subtropical climate. J. Geophys. Res. Biogeosci. 122 (7), 1597-1614. https://doi.org/10.1002/2017JG003805

Xiao, Q.T., Hu, Z.H., Fu, C.S., Bian, H., Lee, X.H., Chen, S.T., Shang, D.Y., 2019. Surface nitrous oxide concentrations and fl uxes from water bodies of the agricultural watershed in Eastern China. Environ. Pollut. 251, 185-192. https://doi.org/10.1016/j.envpol.2019.04.076

Xiao, W., Liu, S.D., Li, H.C., Xiao, Q., Wang, W., Hu, Z.H., Hu, C., Gao, Y.Q., Shen, J., Zhao, X.Y., Zhang, M., Lee, X.H., 2014. A flux-gradient system for simultaneous measurement of the CH_4, CO_2, and H_2O fluxes at a lake-air interface. Environ. Sci. Technol. 48, 14490-14498. https://doi.org/10.1021/es5033713

Xing, Y., Xie, P., Yang, H., Ni, L., Wang, Y., Tang, W., 2004. Diel variation of methane fluxes in summer in a eutrophic subtropical lake in China. J. Freshwa. Ecol. 19, 639-644. https://doi.org/10.1080/02705060.2004.9664745

Yan, F., Sillanpää, M., Kang, S., Aho, K. S.,Qu, B., Wei, D., et al. (2018). Lakes on theTibetan Plateau as conduits ofgreenhouse gases to the atmosphere. J. Geophys. Res.-Biogeo. 123, 2091-2103. https://doi.org/10.1029/2017JG004379

748 Yang, H., Xie, P., Ni, L.Y., Flower, R.J., 2011. Underestimation of CH_4 emission from freshwater
749 lakes in China. Environ. Sci. Technol.45(10), 4203-4204. https://doi.org/10.1021/es2010336
750 Yang, P., Bastviken, D., Jin, B.S., Mou, X.J., Tong, C., 2017a. Effects of coastal marsh conversion
751 to shrimp aquaculture ponds on CH_4 and N_2O emissions. Estuar. Coast. Shelf S. 199,
752 125-131.https://doi.org/10.1016/j.ecss.2017.09.023.
753 Yang, P., He, Q.H., Huang, J.F., Tong, C., 2015. Fluxes of greenhouse gases at two different
754 aquaculture ponds in the coastal zone of southeastern China. Atmos. Environ. 115,
755 269-277.https://doi.org/10.1016/j.atmosenv.2015.05.067
756 Yang, P., Lai, D.Y.F., Jin, B.S., Bastviken, D., Tan, L.S., Tong, C., 2017b. Dynamics of dissolved
757 nutrients in the aquaculture shrimp ponds of the Min River estuary, China: Concentrations,
758 fluxes and environmental loads. Sci. Total Environ. 603-604,
759 256-267.https://doi.org/10.1016/j.scitotenv.2017.06.074
760 Yang, P., Zhang, Y., Yang, H., Zhang, Y. F., Xu, J., Tan, L.S., Tong, C., Lai, D.Y.F., 2019. Large
761 fine-scale spatiotemporal variations of CH_4 diffusive fluxes from shrimp aquaculture ponds
762 affected by organic matter supply and aeration in Southeast China. J. Geophys. Res.-Biogeo.
763 124, 1290-1307. https://doi.org/10.1029/2019JG005025
764 Yang, P., Zhang, Y., Bastviken, D., Lai, D.Y.F., Yang, H., Zhang, Y.F., Guo, Q.Q., Tan, L.S.,
765 Tong, C., 2020. Large increase in diffusive greenhouse gas fluxes from subtropical shallow
766 aquaculture ponds during the passage of typhoons. J. Hydrol. 583, 124643.
767 https://doi.org/10.1016/j.jhydrol.2020.124643
768 Yuan, J. J., Xiang, J., Liu, D. Y., Kang, H., He, T. H., Kim, S., et al. (2019). Rapid growth in
769 greenhouse gas emissions from the adoption of industrial-scale aquaculture. Nat.Clim. Chang.
770 9(4), 318-322. https://doi.org/10.1038/s41558-019-0425-9
771 Zappa, C.J., McGillis, W.R., Raymond, P.A., Edson, J.B., Hintsa, E.J., Zemmelink, H.J., Dacey,
772 J.W.H., Ho, D.T., 2007. Environmental turbulent mixing controls on air-water gas exchange in
773 marine and aquatic systems. Geophys. Res. Lett. 34(10), L10601.
774 https://doi.org/10.1029/2006GL028790
775 Zhang, Y.F., Yang, P., Yang, H., Tan, L.S., Guo, Q.Q., Zhao, G.H., Li, L., Gao, Y.C., Tong, C., 2019.
776 Plot-scale spatiotemporal variations of CO_2 concentration and flux across water-air interfaces
777 at aquaculture shrimp ponds in a subtropical estuary. Environ. Sci. Pollut. R. 26, 5623-5637.
778 https://doi.org/10.1007/s11356-018-3929-3

779 Zhao, J.Y., Zhang, M., Xiao, W., Wang, W., Zhang, Z., Yu, Z., Xiao,Q.T., Cao, Z.D., Xu, J.Z.,
780 Zhang, X.F., Liu, S.D., Lee, X.H., 2019. An evaluation of the flux-gradient and the eddy
781 covariance method to measure CH_4, CO_2, and H_2O fluxes from small ponds. Agr. Forest
782 Meteorol. 275, 255-264. https://doi.org/10.1016/j.agrformet.2019.05.032
783 Zhao, Y., Wu, B. F., Zeng, Y., 2013. Spatial and temporal patterns of greenhouse gas emissions
784 from Three Gorges Reservoir of China. Biogeosciences 10, 1219-1230.
785 https://doi.org/10.5194/bg-10-1219-2013
786 Zhu, D., Wu, Y., Chen, H., He, Y. X., Wu, N., 2016. Intense methane ebullition from open water
787 area of a shallow peatland lake on the eastern Tibetan Plateau. Sci. Total Environ. 542, 57-64.
788 https://doi.org/10.1016/j.scitotenv.2015.10.087

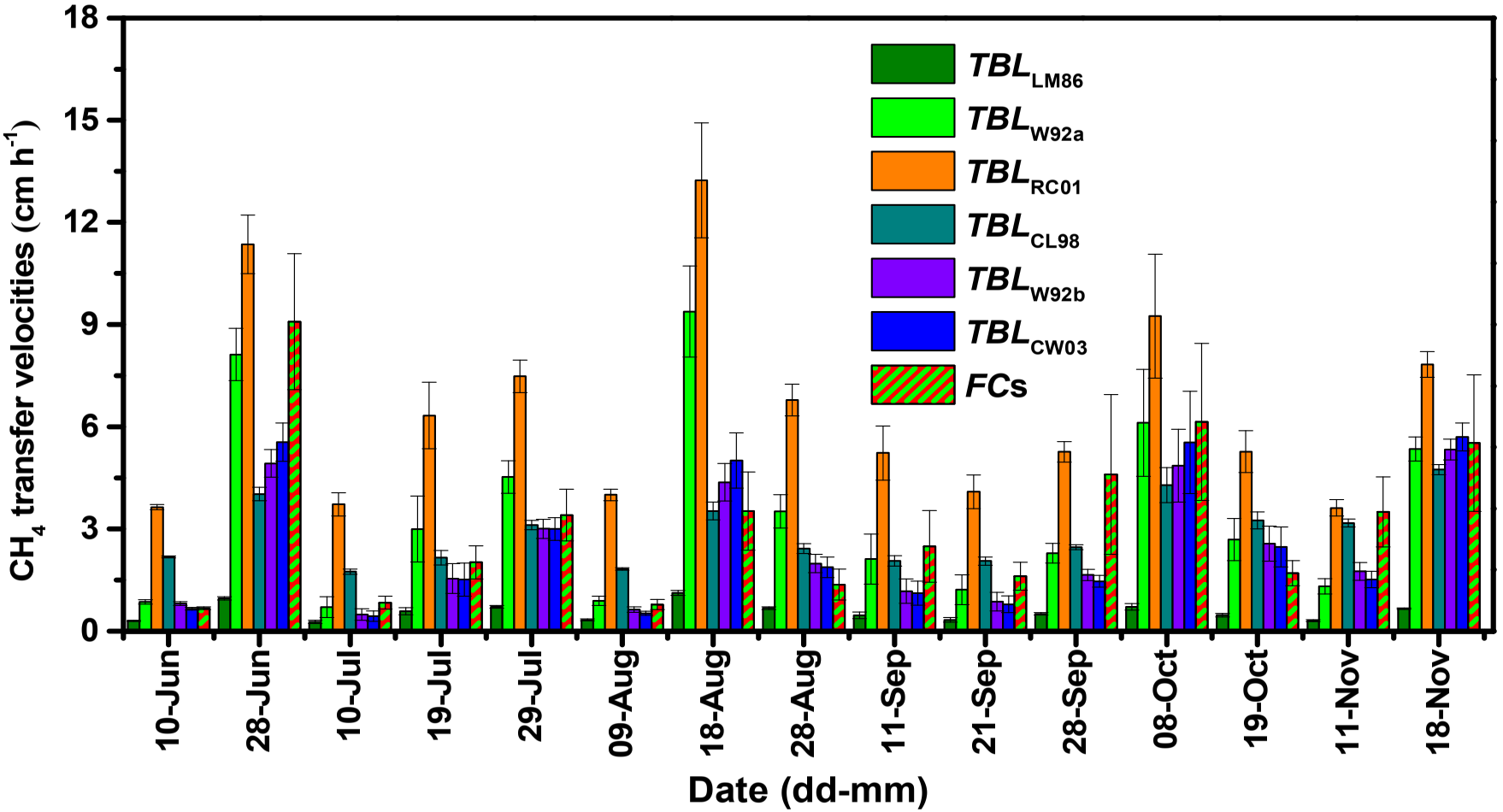

Figure 1. Temporal variation in CH_4 transfer velocities from the aquaculture ponds during the aquaculture period in the Min River Estuary. Values represent the means of nine replicates samples, while the vertical lines indicate standard errors .

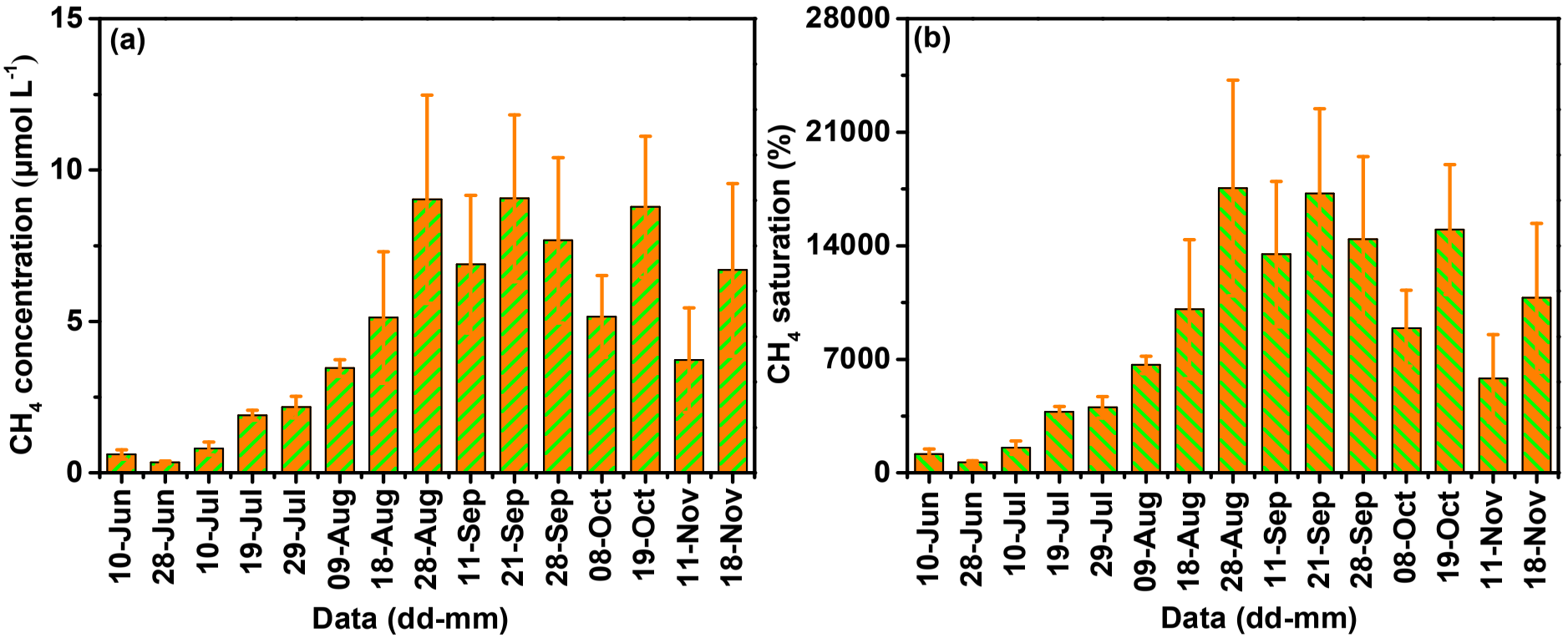

Figure 2. Temporal variation in (a) CH_4 concentration and (b) CH_4 saturation in the surface water (20 cm depth) of the aquaculture ponds in the Min River Estuary during the aquaculture period. Values represent the means of nine replicates samples, while the vertical lines indicate standard errors.

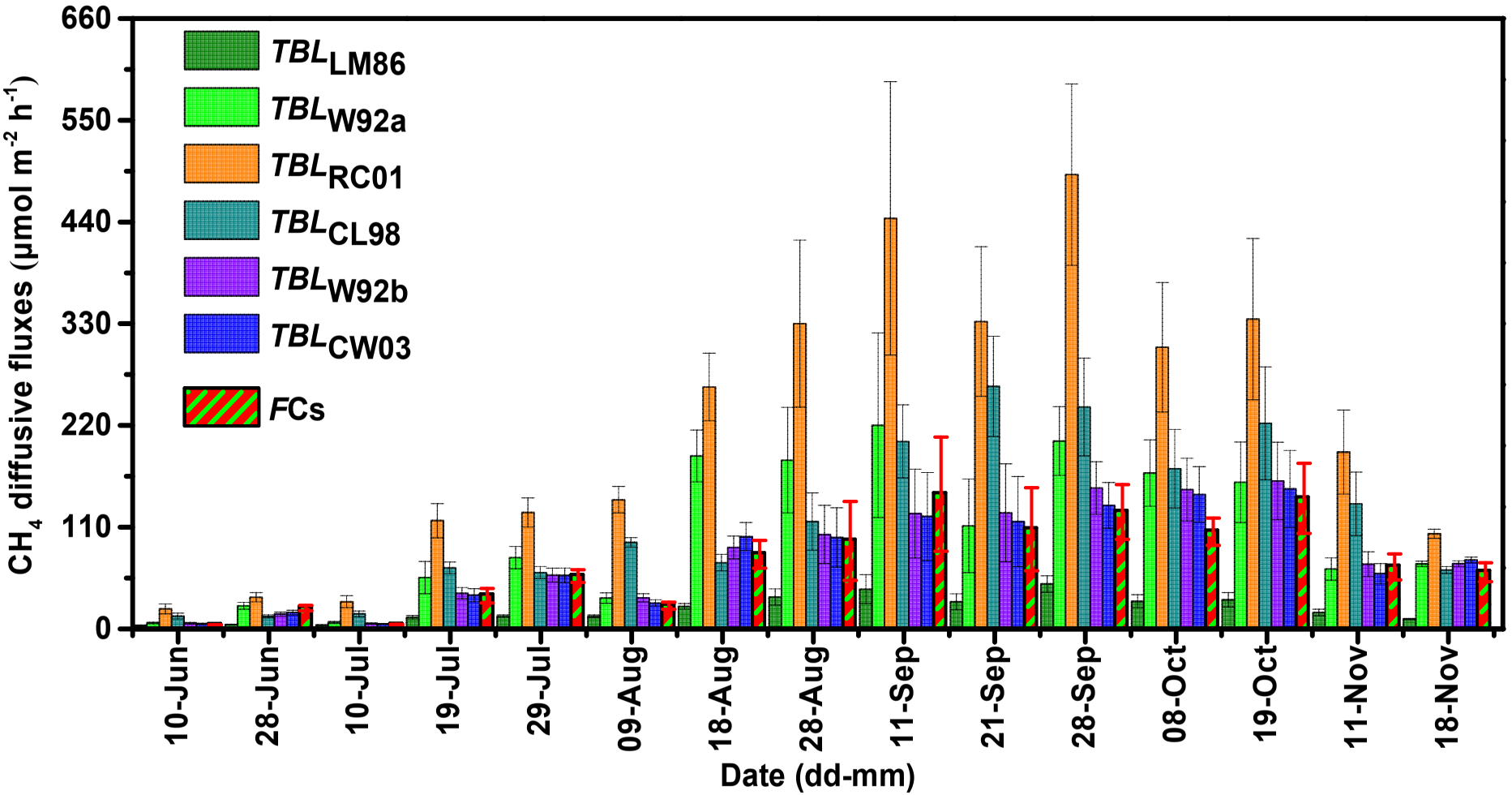

Figure 3. Temporal variation in CH_4 diffusive fluxes measured with the floating chamber method and the gas transfer velocity model methods during the aquaculture period from the aquaculture ponds in the Min River Estuary. Values represent the means of nine replicates samples, while the vertical lines indicate standard errors.

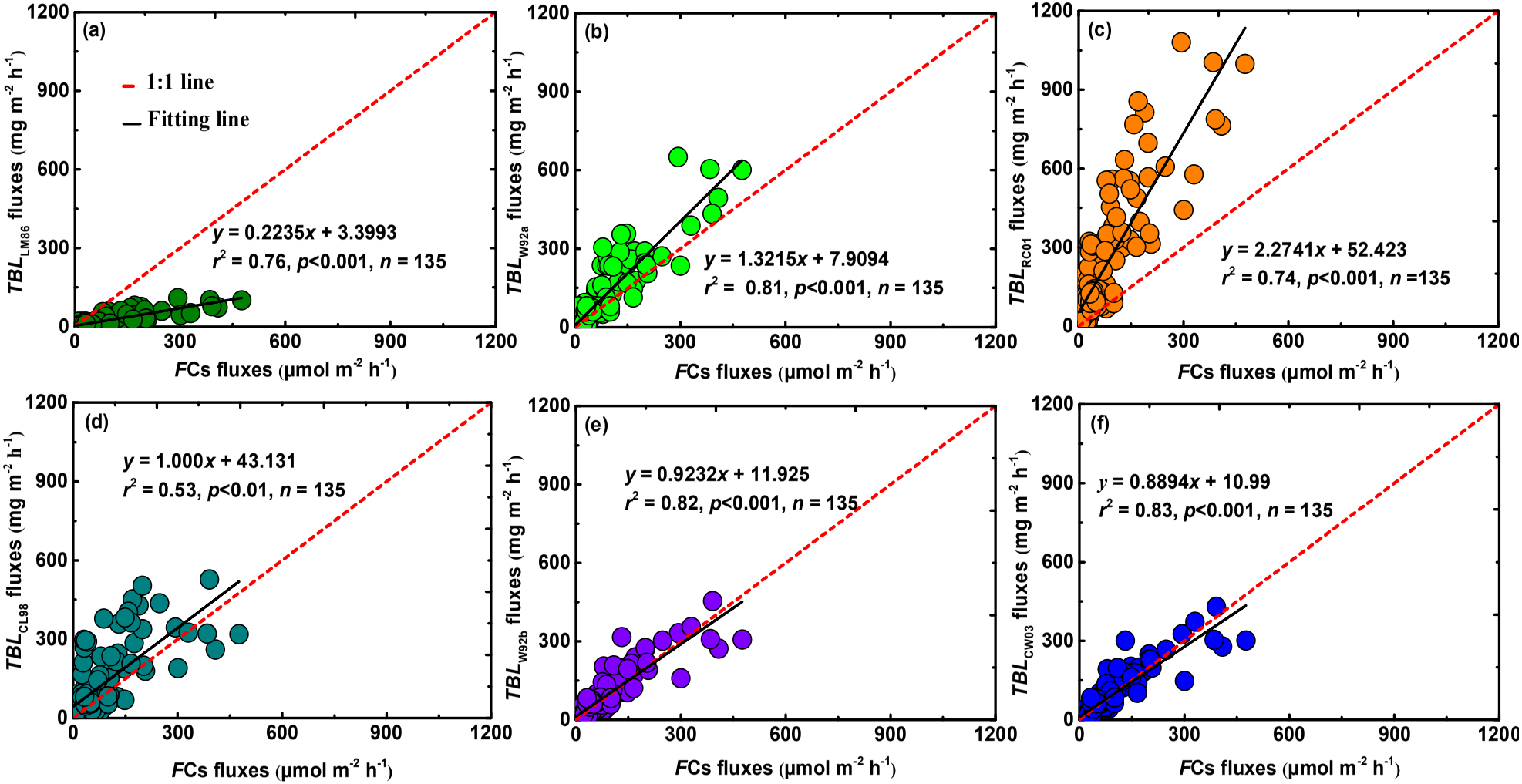

Figure 4. Comparison of CH_4 diffusive flux measured by using the *FCs* method and *TBL* models. Regression equation, linear correlation (r^2) and significance (p) are also shown. Parameter bounds on the regression coefficients are 95% confidence intervals.

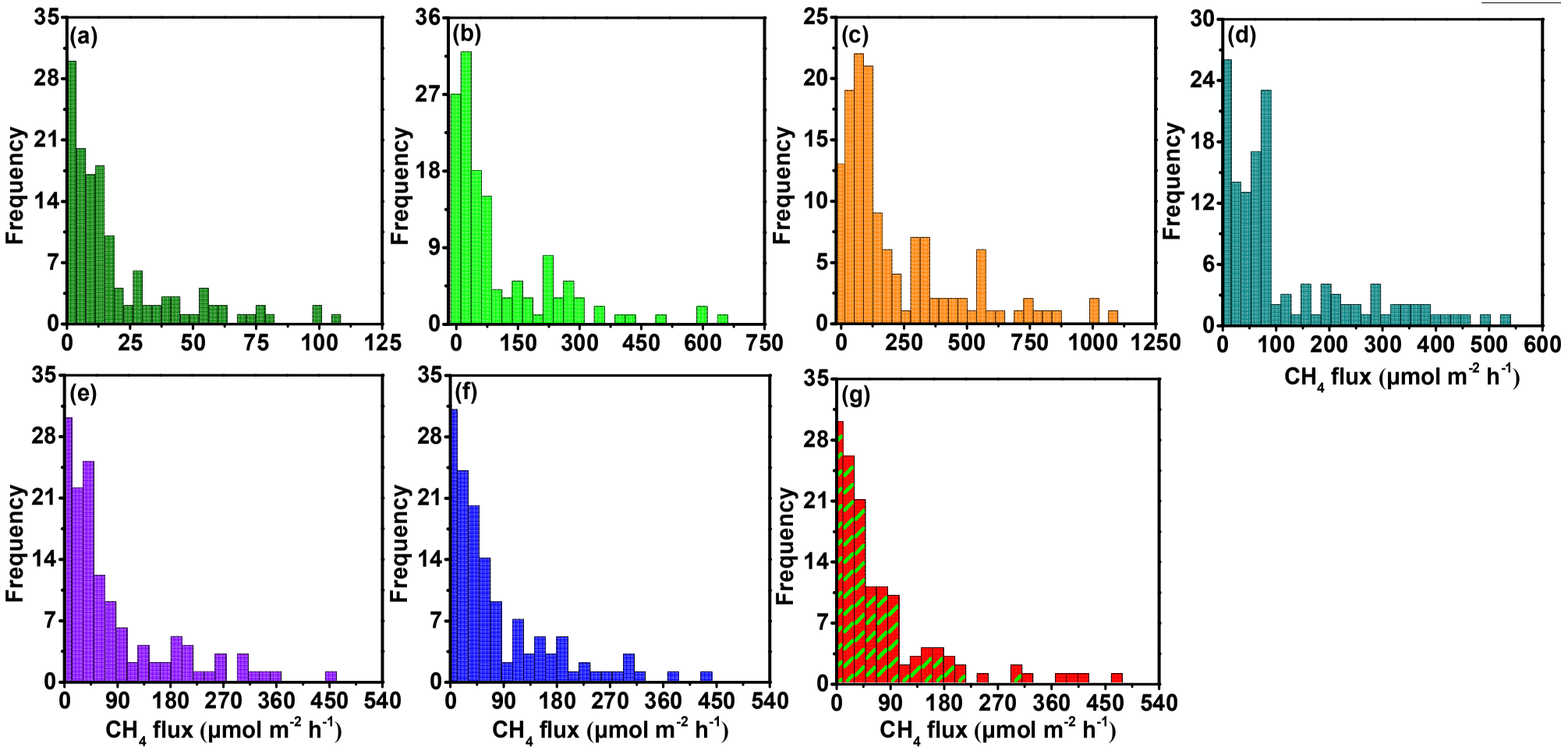

Figure 5. Frequency distribution of CH_4 diffusive fluxes from (a) TBL_{LM86}, (b) TBL_{W92a}, (c) TBL_{RC01}, (d) TBL_{CL98}, (e) TBL_{W92b}, (f) $TBL_{CW03,}$ and (g) FCs measurements at the aquaculture ponds in the Min River Estuary during the aquaculture period.

Table 1

Summary of the *TBL* and *FCs* methods applied to measure CH_4 diffusive fluxes from the aquaculture ponds in Min River Estuary during the aquaculture period.

	***TBL* methods**						***FCs* method**
	TBL_{LM86}	TBL_{W92a}	TBL_{RC01}	TBL_{CL98}	TBL_{W92b}	TBL_{CW03}	
Minimum (μmol m^{-2} h^{-1})	0.6	1.3	5.6	1.9	1.9	1.3	1.3
Maximum (μmol m^{-2} h^{-1})	108.8	650.0	1079.4	527.5	454.4	428.8	476.3
Average (μmol m^{-2} h^{-1})	19.4	103.1	215.6	115.0	78.1	75.0	71.9
Standard deviation	23.1	130.6	236.3	122.5	91.3	86.9	88.8
Coefficient of variation	1.18	1.27	1.09	1.06	1.16	1.15	1.24

Table 2

Pearson correlation coefficients for dissolved CH_4 concentration, CH_4 diffusive fluxes and environmental variables from the aquaculture ponds in Min River Estuary during the aquaculture period[a]. Bold numbers denote correlation coefficients for significant relationships.

Environmental variables	Dissolved CH_4 concentration	CH_4 diffusive fluxes
Meteorological parameters		
Air temperature	**0.214***	**0.203***
Wind speed (W_S)	NS	**0.281***
Atmospheric pressure	NS	NS
Water parameters		
Water temperature	NS	NS
Dissolved oxygen (DO)	NS	NS
TOC concentration	**0.312****	**0.296****
NO_3^--N concentration	**-0.401****	**-0.392****
Electrical conductivity (EC)	**-0.361****	**-0.185***

[a] The symbols * and ** indicate significant correlations at the 0.05 and 0.01 levels, respectively. n = 135 for environmental variables and CH_4 diffusive fluxes from the aquaculture ponds. CH_4 diffusive fluxes were directly measured using floating chambers method.

Supporting Information

Title: Diffusive CH_4 fluxes from aquaculture ponds using floating chambers and thin boundary layer equations

Ping Yang[a,b,1], Jiafang Huang[a,b,1], Hong Yang[c,d,e,1], Josep Peñuelas[f,g], Kam W. Tang[h], Derrick Y.F. Lai[i*], Dongqi Wang[j], Qitao Xiao[k], Jordi Sardans[f,g,], Yifei Zhang[a,b], Chuan Tong[a,b,***]**

[a]*Key Laboratory of Humid Subtropical Eco-geographical Process of Ministry of Education, Fujian Normal University, Fuzhou 350007, P.R. China*

[b]*School of Geographical Sciences, Fujian Normal University, Fuzhou 350007, P.R. China*

[c]*College of Environmental Science and Engineering, Fujian Normal University, Fuzhou 350007, P.R. China*

[d]*Collaborative Innovation Center of Atmospheric Environment and Equipment Technology, Jiangsu Key Laboratory of Atmospheric Environment Monitoring and Pollution Control (AEMPC), School of Environmental Science and Engineering, Nanjing University of Information Science and Technology, Nanjing 210044, China;*

[e]*Department of Geography and Environmental Science, University of Reading, Reading RG6 6AB, U.K.*

[f]*CSIC, Global Ecology Unit CREAF-CSIC-UAB, Bellaterra, Catalonia, Spain*

[g]*CREAF, Cderdanyola del Vallès, Catalonia, Spain*

[h]*Department of Biosciences, Swansea University, Swansea SA2 8PP, U. K.*

[i]*Department of Geography and Resource Management, The Chinese University of Hong Kong, Shatin, New Territories, Hong Kong SAR, China*

[j]*School of Geographical Sciences, East China Normal University, Shanghai 200241, China*

[k]*Key Laboratory of Watershed Geographic Sciences, Nanjing Institute of Geography and Limnology, Chinese Academy of Sciences, Nanjing, 210008, China*

***Correspondence to:** Derrick Y.F. Lai

Email: dyflai@cuhk.edu.hk

***Correspondence to:** Jordi Sardans

Email: j.sardans@creaf.uab.cat

****Correspondence to:** Chuan Tong

Email: tongch@fjnu.edu.cn

[1]Ping Yang, Jiafang Huang, and Hong Yang contributed equally to this work.

Supporting Information Summary

No. of pages: 16 No. of figures: 4 No. of tables: 5

Page S5: Figure S1. Location of the study area and sampling sites at aquaculture ponds in Min River Estuary, Southeast China.

Page S6: Figure S2. Schematic diagram for the gas sampling device of CH_4 diffusive flux across the water-air interface. Numbers 1, 2, 3, 4, 5, 6, 7, 8, 9, 10, 11, and 12 represents chambers body, Neoprene floats, thin gauze, mooring anchor, sampling tube, 60-mL plastic syringes equipped with three-way stopcocks, fixed rope, valve body, valve body, gas collecting hole, ribbon, and handle, respectively.

Page S7: Figure S3. (a) Temporal variation in the wind speed (W_S), and (b) frequency distribution of wind speed at the shrimp ponds in the Min River Estuary during the aquaculture period.

Page S8: Figure S4. Temporal variation in (a) water temperature, (b) dissolved oxygen, (c) TOC, and (b) $N\text{-}NO_x^-$ in the surface water (20 cm depth) of the aquaculture ponds in the Min River Estuary during the aquaculture period. *Error bars* represent standard error (n = 9). Data are after Yang et al. [*unpublished data*] for reference and review only.

Page S9: Figure S5. Boxplots of CH_4 diffusive fluxes estimated using the *TBL* and *FCs* methods at the aquaculture ponds in Min River Estuary during the aquaculture period. The letters above the boxes represent the LSD (Least Significant Difference) test results, and different letters mean significant difference at 0.05 level. The centre line and square represent the median value and area-weighted average.

Page S10: Figure S6. Comparison of CH_4 fluxes measured using the *FCs* with gauze (*FCs*-G) and without gauze (*FCs*-NG) from the aquaculture ponds in the Min River Estuary during the aquaculture period. Data are after Yang et al. [*unpublished data*] for reference and review only. Values represent the means of nine replicates samples, while the vertical lines indicate standard errors.

Page S11: Table S1. Characteristics of the three aquaculture ponds in the Min River Estuary.

Page S12: Table S2. The best GLS model (lowest AIC values) with the CH_4 fluxes as functions of environmental values.

Page S15: Table S3. Pearson correlation coefficients for environmental variables, dissolved CH_4 concentration and CH_4 diffusive fluxes from the aquaculture ponds in Min River Estuary during the aquaculture period.

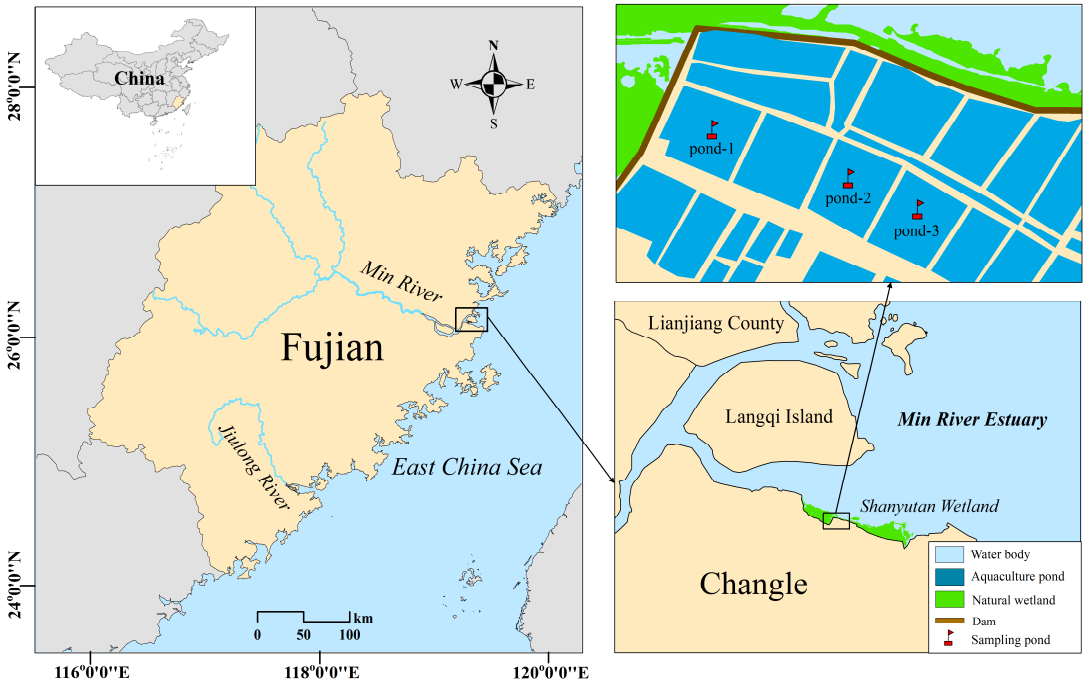

67

68 **Figure S1.** Location of the study area and sampling sites at aquaculture ponds in Min

69 River Estuary, Southeast China.

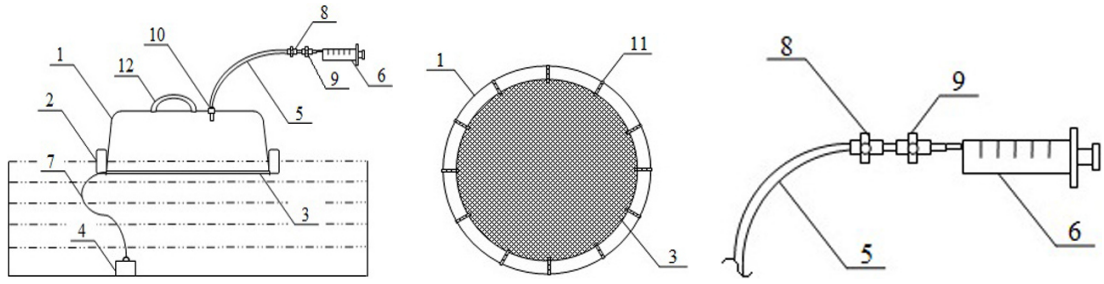

Figure S2. Schematic diagram for the gas sampling device of CH_4 diffusive flux across the water-air interface. Numbers 1, 2, 3, 4, 5, 6, 7, 8, 9, 10, 11, and 12 represents chambers body, Neoprene floats, thin gauze, mooring anchor, sampling tube, 60-mL plastic syringes equipped with three-way stopcocks, fixed rope, valve body, valve body, gas collecting hole, ribbon, and handle, respectively.

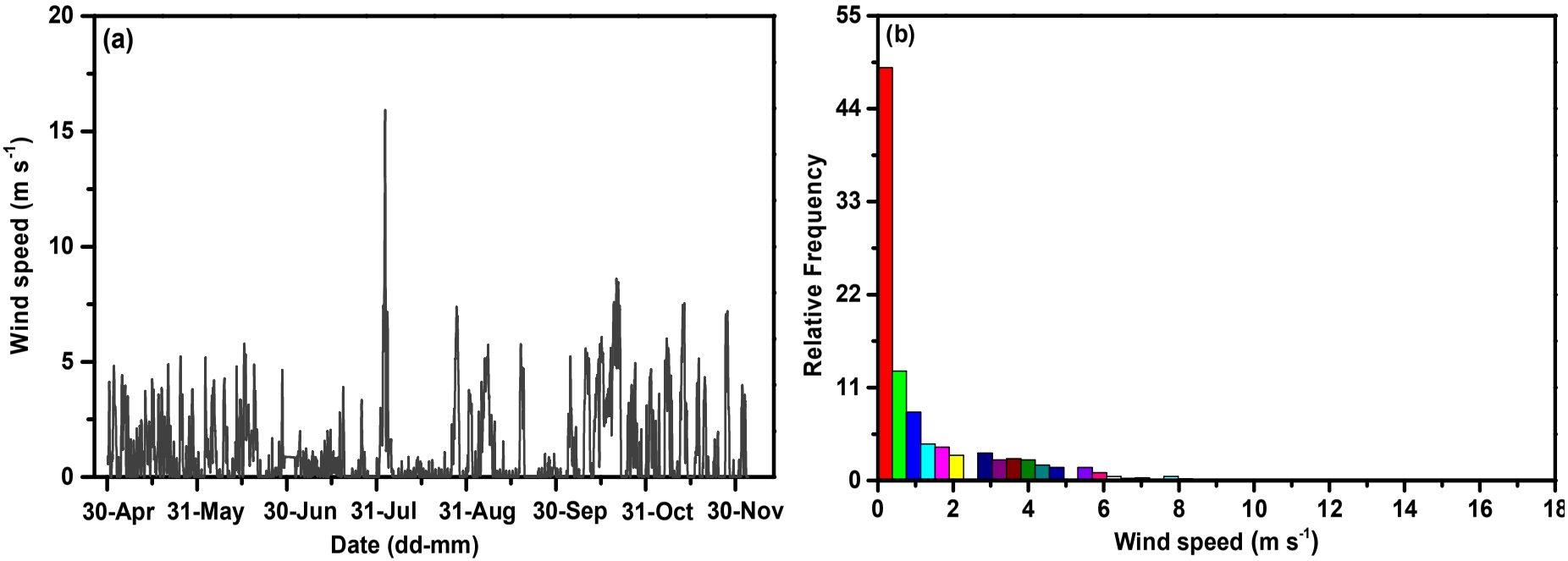

Figure S3. (a) Temporal variation in the wind speed (W_S), and (b) frequency distribution of wind speed at the shrimp ponds in the Min River Estuary during the aquaculture period.

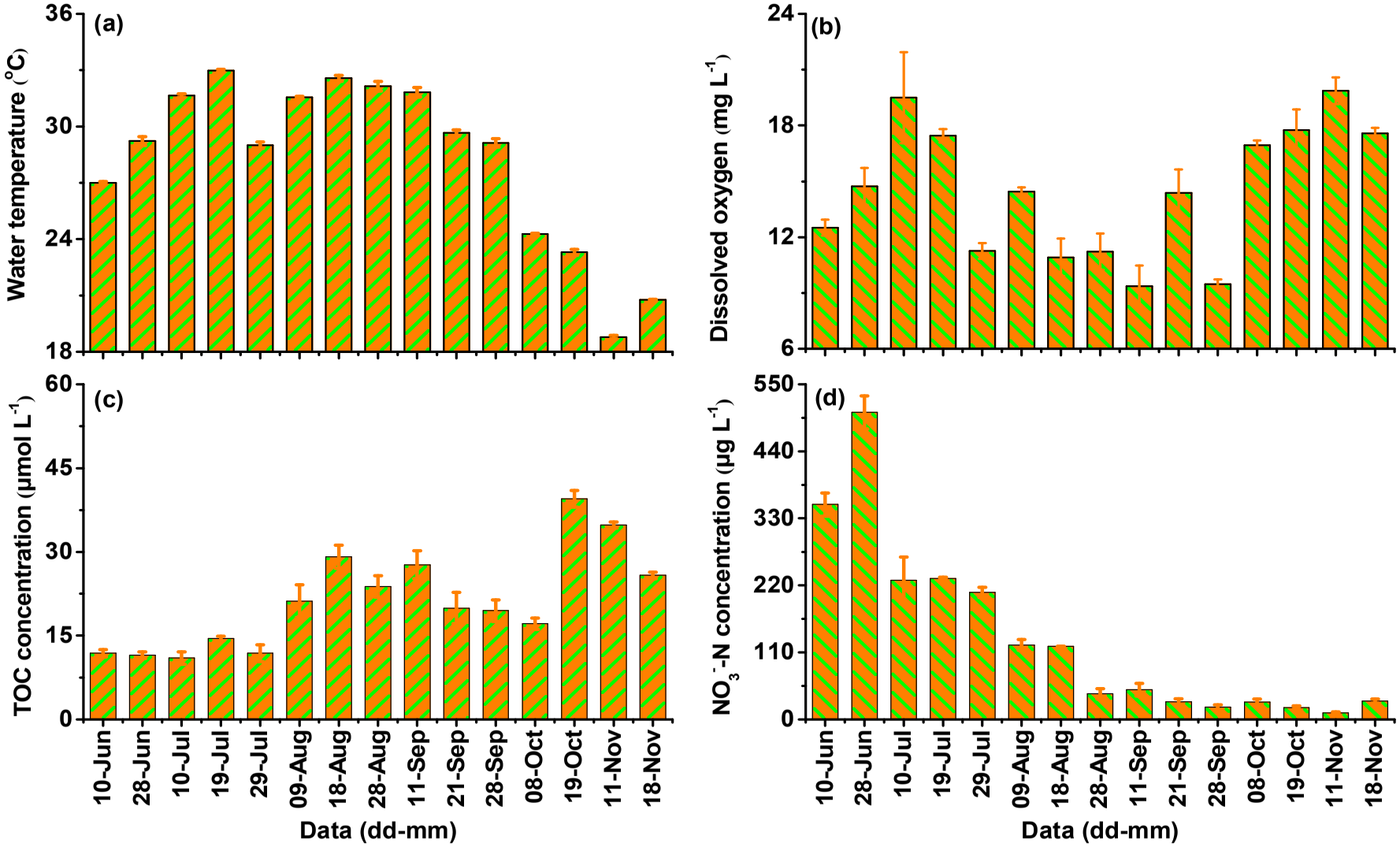

Figure S4. Temporal variation in (a) water temperature, (b) dissolved oxygen, (c) TOC, and (b) NO_3^--N in the surface water (20 cm depth) of the aquaculture ponds in the Min River Estuary during the aquaculture period. *Error bars* represent standard error (n = 9). Data are after Yang et al. [*unpublished data*] for reference and review only.

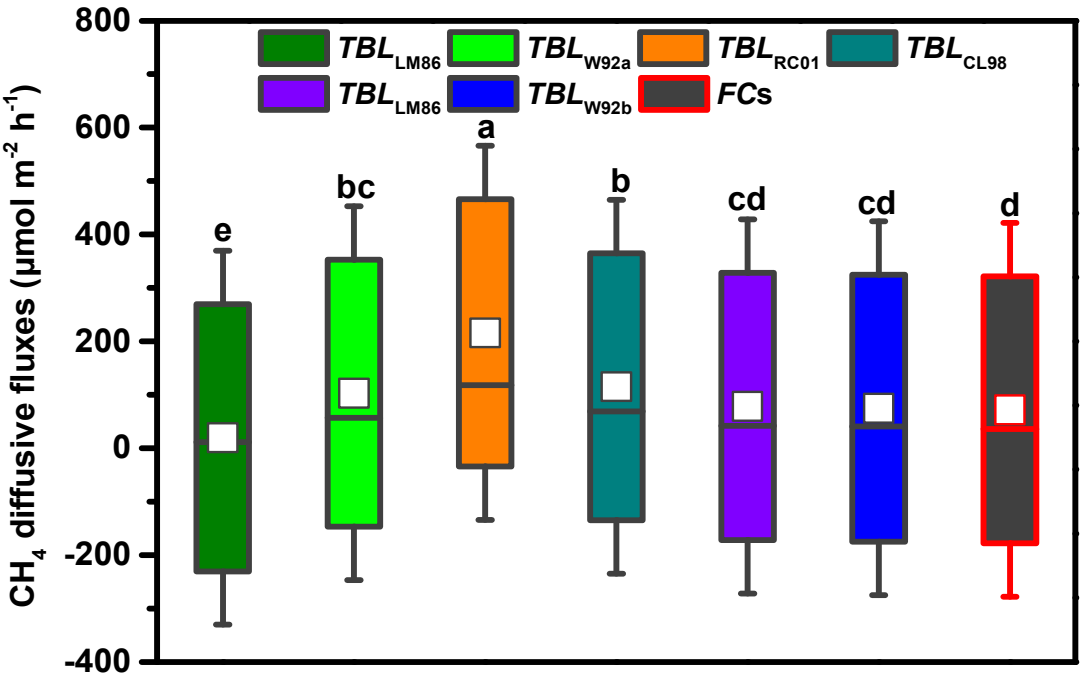

Figure S5. Boxplots of CH_4 diffusive fluxes estimated using the *TBL* and *FCs* methods at the aquaculture ponds in Min River Estuary during the aquaculture period. The letters above the boxes represent the LSD (Least Significant Difference) test results, and different letters mean significant difference at 0.05 level. The centre line and square represent the median value and area-weighted average.

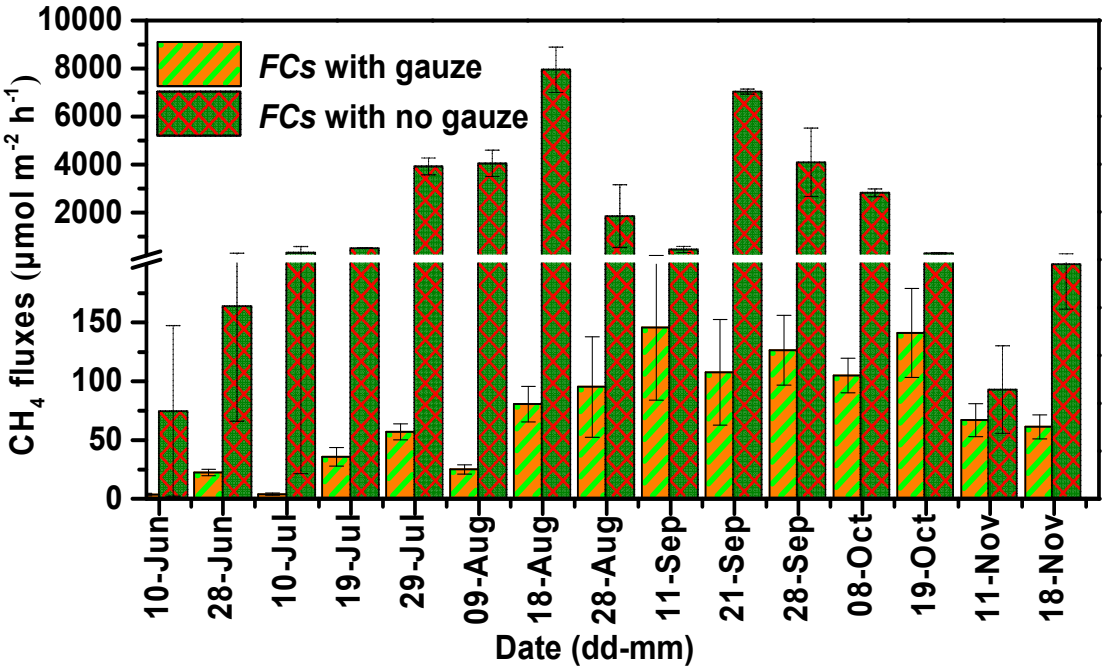

Figure S6. Comparison of CH_4 fluxes measured using the *FCs* with gauze (*FCs*-G) and without gauze (*FCs*-NG) from the aquaculture ponds in the Min River Estuary during the aquaculture period. Data are after Yang et al. [*unpublished data*] for reference and review only. Values represent the means of nine replicates samples, while the vertical lines indicate standard errors.

Table S1 Characteristics of the three aquaculture ponds in the Min River Estuary. *.

Parameters	Pond-I	Pond-II	Pond-III
Shrimp species	*Litopenaeus vannamei*	*Litopenaeus vannamei*	*Litopenaeus vannamei*
Water depth (m)	1.3 (0.3 – 1.7)	1.7 (0.5 – 2.1)	1.5 (0.3 – 1.8)
Water salinity (‰)	3.6 (1.5 – 6.8)	2.2 (1.7 – 5.2)	2.8 (1.7 – 5.4)
Surface area (m^2)	21426.94	18412.89	19112.71
Stocking density (PL m^{-2})[a]	150	120	119
Survival rate (%)[a]	45	62	59
Feed conversion rate[b]	3.5	2.3	2.5

* Based on Zhang et al. (2019).

[a] The data for the stocking density, survival rate, and yield were provided by the farmers; [b] Feed conversion rate = dry weight of feeds added / wet weight of shrimps produced.

Table S2 The best GLS model (lowest AIC values) with the CH_4 fluxes as functions of environmental values.

Variables			
	Model	Model R^2 and P-value	Model independent factors statistics
TBL_{LM86}	gls(CH4flux ~ disCH4 + U10 + watertemp + NO3N, data=dades, method ="REML")	R^2=0.47 P<0.0001	Coefficients: Estimate / Std. Error / t-value / p-value (Intercept) -0.396 / 0.166 / -2.38 / 0.019 disCH4 0.0300 / 0.00399 / 7.54 / <0.0001 U10 0.0515 / 0.0167 / 3.08 / 0.0025 watertemp 0.0187 / 0.00553 / 3.39 / 0.00093 NO3N -0.786 / 0.178 / -4.41 / <0.0001
TBL_{W92a}	gls(CH4flux ~ disCH4 + U10 + watertemp + NO3N, data=dades, method ="REML")	R^2=0.50 P<0.0001	Coefficients: Estimate / Std. Error / t-value / p-value (Intercept) -3.52 / 0.945 / -3.73 / <0.0001 disCH4 0.141 / 0.0227 / 6.20 / <0.0001 U10 0.614 / 0.0951 / 6.45 / <0.0001 watertemp 0.122 / 0.0314 / 3.89 / <0.0001 NO3N -4.64 / 1.014 / -4.58 / <0.0001
TBL_{RC01}	gls(CH4flux ~ disCH4 + U10 + watertemp + NO3N, data=dades, method ="REML")	R^2=0.54 P<0.0001	Coefficients: Estimate / Std. Error / t-value / p-value (Intercept) -3.32 / 1.64 / -2.03 / 0.045 disCH4 0.331 / 0.0393 / 8.42 / <0.0001 U10 0.464 / 0.165 / 2.81 / 0.0057 watertemp 0.178 / 0.0546 / 3.26 / 0.0014 NO3N -8.18 / 1.76 / -4.65 / <0.0001
TBL_{CL98}	gls(CH4flux ~ disCH4 + NO3N, data=dades,	R^2=0.53	Coefficients:

	method ="REML")	P<0.0001		Estimate	Std. Error	t-value	p-value
			(Intercept)	1.45	0.212	6.86	<0.0001
			disCH4	0.181	0.0203	8.95	<0.0001
			NO3N	-3.59	0.862	-4.16	<0.0001
TBL_{W92b}	gls(CH4flux ~ disCH4 + U10 + NO3N, data=dades, method ="REML")	R^2=0.46 P<0.0001	Coefficients:				
				Estimate	Std. Error	t-value	p-value
			(Intercept)	0.348	0.244	1.43	0.16
			disCH4	0.108	0.0163	6.61	<0.0001
			U10	0.287	0.0676	4.24	<0.0001
			NO3N	-2.90	0.695	-4.18	0.0001
TBL_{CW03}	gls(CH4flux ~ disCH4 + U10 + NO3N, data=dades, method ="REML")	R^2=0.48 P<0.0001	Coefficients:				
				Estimate	Std. Error	t-value	p-value
			(Intercept)	0.178	0.230	0.774	0.44
			disCH4	0.0988	0.0153	6.46	<0.00019
			U10	0.340	0.0634	5.35	<0.0001
			NO3N	-2.79	0.652	-4.27	<0.0001
FCs	gls(CH4flux ~ disCH4 + U10 + NO3N, data=dades, method ="REML")	R^2=0.35 P<0.0001		Estimate	Std. Error	t-value	p-value
			(Intercept)	0.258	0.263	0.98	0.33
			disCH4	0.0784	0.0175	4.47	<0.0001
			U10	0.324	0.0728	4.46	<0.0001
			NO3N	-2.71	0.748	-3.63	0.00041

Table S3 Pearson correlation coefficients for environmental variables, dissolved CH_4 concentration and CH_4 diffusive fluxes from the aquaculture ponds in Min River Estuary during the aquaculture period.

Environmental variables	**CH_4 diffusive fluxes**					
	***TBL*$_{LM86}$**	***TBL*$_{W92a}$**	***TBL*$_{RC01}$**	***TBL*$_{CL98}$**	***TBL*$_{W92b}$**	***TBL*$_{CW03}$**

Meteorological parameters						
Air temperature	NS	**0.176***	NS	**0.224****	**0.253****	**0.254****
U_{10}	NS	NS	NS	NS	NS	NS
Atmospheric pressure	NS	NS	NS	NS	NS	NS
Water parameters						
Water temperature	NS	NS	NS	NS	NS	NS
Dissolved oxygen (DO)	NS	NS	NS	NS	NS	NS
TOC concentration	**0.301****	**0.328****	**0.306****	**0.263****	**0.347****	**0.355****
NO_3^--N concentration	**-0.439****	**-0.384****	**-0.464****	**-0.502****	**-0.455****	**-0.444****
CH_4 concentration	**0.619****	**0.522****	**0.659****	**0.688****	**0.572****	**0.553****
Gas transfer velocity (k_x)	NS	NS	NS	NS	NS	NS

The symbols * and ** indicate significant correlations at the 0.05 and 0.01 levels, respectively. NS indicates non-significant.

References

Zhang, Y.F., Yang,P., Yang,H., Tan,L.S., Guo,Q.Q., Zhao,G.H., Li,L., Gao, Y.C., Tong, C., 2019. Plot-scale spatiotemporal variations of CO_2 concentration and flux across water-air interfaces at aquaculture shrimp ponds in a subtropical estuary. Environ. Sci. Pollut. R. 26, 5623-5637. https://doi.org/10.1007/s11356-018-3929-3